34. Motion Control of Wheeled Mobile Robots

Pascal Morin, Claude Samson

This chapter may be seen as a follow up to Chap. 17, devoted to the classification and modeling of basic wheeled mobile robot (WMR) structures, and a natural complement to Chap. 35, which surveys motion planning methods for WMRs. A typical output of these methods is a feasible (or admissible) reference state trajectory for a given mobile robot, and a question which then arises is how to make the physical mobile robot track this reference trajectory via the control of the actuators with which the vehicle is equipped. The object of the present chapter is to bring elements of the answer to this question based on simple and effective control strategies. A first approach would consist in applying *open-loop* steering control laws like those developed in Chap. 35. However, it is well known that this type of control is not robust to modeling errors (the sources of which are numerous) and that it cannot guarantee that the mobile robot will move along the desired trajectory as planned. This is why the methods here presented are based on *feedback* control. Their implementation supposes that one is able to measure the variables involved in the control loop (typically the position and orientation of the mobile robot with respect to either a fixed frame or a path that the vehicle should follow). Throughout this chapter we will assume that these measurements are available continuously in time and that they are not corrupted by noise. In a general manner, robustness considerations will not be discussed in detail, one reason being that, beyond imposed space limitations, a large part of the presented approaches are based on linear control theory. The feedback control laws then inherit the strong robustness properties associated with stable linear systems.

Results can also be subsequently refined by using complementary, eventually more elaborate, automatic control techniques.

34.1 Background

The control of wheeled mobile robots has been, and still is, the subject of numerous research studies. In particular, nonholonomy constraints associated with these systems have motivated the development of highly nonlinear control techniques. These approaches are addressed in the present chapter, but their exposition is deliberately limited in order to give priority to more classical techniques whose bases, both practical and theoretical, are better established.

For the sake of simplicity, the control methods are developed mainly for unicycle-type and car-like mobile robots, which correspond respectively to the types (2, 0) and (1, 1) in the classification proposed in Chap. 17. Most of the results can in fact be extended/adapted to other mobile robots, in particular to systems with trailers. We will mention the cases where such extensions are straightforward. All reported simulation results, illustrating various control problems and solutions, are carried out for a car-like vehicle, whose kinematics is slightly more complex than that of unicycle-type vehicles.

Recall (Fig. 34.1) that:

1. A *unicycle-type mobile robot* is schematically composed of two independent actuated wheels on a common axle whose direction is rigidly linked to the robot chassis, and one or several passively orientable – or caster – wheels, which are not controlled and serve for sustentation purposes.
2. A (rear-drive) *car-like mobile robot* is composed of a motorized wheeled axle at the rear of the chassis, and one (or a pair of) orientable front steering wheel(s).

Note also, as illustrated by the diagram below (Fig. 34.2), that a car-like mobile robot can be viewed (at least kinematically) as a unicycle-type mobile robot to which a trailer is attached.

Three generic control problems are studied in this chapter, as described below.

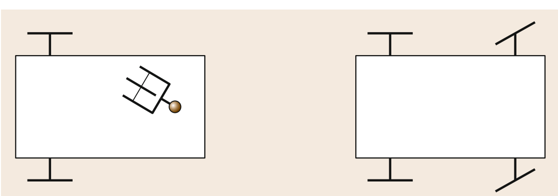

Fig. 34.1 Unicycle-type (*left*) and car-like (*right*) mobile robots

34.1.1 Path Following

Given a curve $\mathcal{C}$ on the plane, a (nonzero) longitudinal velocity v_0 for the robot chassis, and a point P attached to the chassis, the goal is to have the point P follow the curve $\mathcal{C}$ when the robot moves with the velocity v_0. The variable that one has to stabilize at zero is thus the distance between the point P and the curve (i. e., the distance between P and the closest point M on $\mathcal{C}$). This type of problem typically corresponds to driving on a road while trying to maintain the distance between the vehicle chassis and the side of the road constant. Automatic wall following is another possible application.

34.1.2 Stabilization of Trajectories

This problem differs from the previous one in that the vehicle's longitudinal velocity is no longer predetermined because one also aims to monitor the distance gone along the curve $\mathcal{C}$. This objective supposes that the geometric curve $\mathcal{C}$ is complemented with a time schedule, i. e., that it is parameterized with the time variable t. This boils down to defining a trajectory $t \longmapsto (x_r(t), y_r(t))$ with respect to a reference frame $\mathcal{F}_0$. Then the goal is to stabilize the position error vector $(x(t) - x_r(t), y(t) - y_r(t))$ at zero, with $(x(t), y(t))$ denoting the coordinates of point P in $\mathcal{F}_0$ at time t. The problem may also be formulated as one of controlling the vehicle in order to track a reference vehicle whose trajectory is given by $t \longmapsto (x_r(t), y_r(t))$. Note that perfect tracking is achievable only if the reference trajectory is feasible for the physical vehicle, and that a trajectory which is feasible for a unicycle-type vehicle is not necessarily feasible for a car-like vehicle. Also, in addition to monitoring the position $(x(t), y(t))$ of the robot, one may be willing to control the chassis orientation $\theta(t)$ at a desired reference value $\theta_r(t)$ associated with the orientation of the reference vehicle. For a nonholonomic unicycle-type robot, a reference trajectory $(x_r(t), y_r(t), \theta_r(t))$ is feasible if it is produced by a reference vehicle which has the

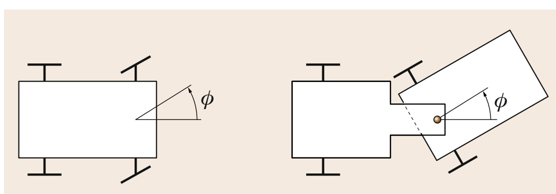

Fig. 34.2 Analogy car/unicycle with trailer

same kinematic limitations as the physical robot. For instance, most trajectories produced by an omnidirectional vehicle (omnibile vehicle in the terminology of Chap. 17) are not feasible for a nonholonomic mobile robot. However, nonfeasibility does not imply that the reference trajectory cannot be tracked in an approximate manner, i. e., with small (although nonzero) tracking errors. This justifies the introduction of the concept of *practical* stabilization, as opposed to *asymptotic* stabilization when the tracking errors converge to zero. The last part of this chapter will be devoted to a recent, and still prospective, control approach for the practical stabilization of trajectories which are not necessarily feasible.

34.1.3 Stabilization of Fixed Postures

Let $\mathcal{F}_1$ denote a frame attached to the robot chassis. In this chapter, we call a robot posture (or situation) the association of the position of a point P located on the robot chassis with the orientation $\theta(t)$ of $\mathcal{F}_1$ with respect to a fixed frame $\mathcal{F}_0$ in the plane of motion. For this last problem, the objective is to stabilize at zero the posture vector $\xi(t) = (x(t), y(t), \theta(t))$, with $(x(t), y(t))$ denoting the position of P expressed in $\mathcal{F}_0$. Although a fixed desired (or reference) posture is obviously a particular case of a feasible trajectory, this problem cannot be solved by classical control methods.

The chapter is organized as follows. Section 34.2 is devoted to the choice of control models and the determination of modeling equations associated with the path-following control problem. In Sect. 34.3, the problems of path following and trajectory stabilization in position are studied under an assumption upon the location of the point P chosen on the robot chassis. This assumption implies that the motion of this point is not constrained. It greatly simplifies the resolution of the considered problems. However, a counterpart of this simplification is that the stability of the robot's orientation is not always guaranteed, in particular during phases when the sign of the robot's longitudinal velocity is not constant. The assumption upon P is removed in Sect. 34.4, and both problems are reconsidered, together with the problem of stabilizing a fixed posture. At the end of this section, a certain number of shortcomings and limitations inherent to the objective of asymptotic stabilization are pointed out. They can be circumvented by considering an objective of practical stabilization instead. Some elements of a recent, and still prospective, control approach developed with this point of view – based on the use of so-called *transverse functions* – are presented in the Sect. 34.4.6. Finally, a few complementary issues on the feedback control of mobile robots are briefly discussed in the concluding Sect. 34.5, with a list of commented references for further reading on WMRs motion control.

34.2 Control Models

34.2.1 Kinematics Versus Dynamics

Relation (17.29) in Chap. 17 provides a general configuration dynamic model for WMRs. Its particularization to the case of unicycle-type and car-like mobile robots gives

$$\boldsymbol{H}(\boldsymbol{q})\dot{\boldsymbol{u}} + \boldsymbol{F}(\boldsymbol{q}, \boldsymbol{u})\boldsymbol{u} = \boldsymbol{\Gamma}(\phi)\boldsymbol{\tau} \tag{34.1}$$

with $\boldsymbol{q}$ denoting a robot's configuration vector, $\boldsymbol{u}$ a vector of independent velocity variables associated with the robot's degrees of freedom, $\boldsymbol{H}(\boldsymbol{q})$ a reduced inertia matrix (which is invertible for any $\boldsymbol{q}$), $\boldsymbol{F}(\boldsymbol{q}, \boldsymbol{u})\boldsymbol{u}$ a vector of forces combining the contribution of Coriolis and wheel–ground contact forces, ϕ the orientation angle of the car's steering wheel, $\boldsymbol{\Gamma}$ an invertible control matrix (which is constant in the case of a unicycle-type vehicle), and $\boldsymbol{\tau}$ a vector of independent motor torques (whose dimension is equal to the number of degrees of freedom in the case of full actuation, i. e., equal to two for the vehicles considered herein). In the case of a unicycle-type vehicle, a configuration vector is composed of the components of the chassis posture vector $\boldsymbol{\xi}$ and the orientation angles of the castor wheels (with respect to the chassis). In the case of a car-like vehicle, a configuration vector is composed of the components of $\boldsymbol{\xi}$ and the steering wheel angle ϕ.

To be complete, this dynamic model must be complemented with kinematic equations in the form (the relation (17.30))

$$\dot{\boldsymbol{q}} = \boldsymbol{S}(\boldsymbol{q})\boldsymbol{u} \tag{34.2}$$

from which one can extract a reduced kinematic model (the relation (17.33))

$$\dot{z} = \boldsymbol{B}(z)\boldsymbol{u} \tag{34.3}$$

with $z = \boldsymbol{\xi}$, in the case of a unicycle-type vehicle, and $z = (\boldsymbol{\xi}, \phi)$ in the case of a car-like vehicle.

In the automatic control terminology, the complete dynamic model (34.1–34.2) forms a *control system* which can be written as $\dot{\boldsymbol{X}} = f(\boldsymbol{X}, \boldsymbol{\tau})$ with $\boldsymbol{X} = (\boldsymbol{q}, \boldsymbol{u})$ denoting the state vector of this system, and $\boldsymbol{\tau}$ the vector of control inputs. The kinematic models (34.2) and (34.3) are also control systems with respective state vectors $\boldsymbol{q}$ and z and control vector $\boldsymbol{u}$. Any of these models can be used for control design and analysis purposes. In the remainder of this chapter, we have chosen to work with the kinematic model (34.3). By analogy with the motion control of manipulator arms, this boils down to using a model with velocity control inputs, rather than a model with torque control inputs. The main reasons for this choice are the following:

1. The kinematic model is simpler than the dynamic one. In particular, it does not involve a certain number of matrix-valued functions whose precise determination relies on the knowledge of numerous parameters associated with the vehicle and its actuators (geometric repartition of constitutive bodies, masses and mass moments of inertia, coefficients of reduction in the transmission of torques produced by the motors, etc.). For many applications, it is not necessary to know all these terms precisely.
2. In the case of robots actuated with electrical motors, these motors are frequently supplied with *low-level* velocity control loops which take a desired angular velocity as input and stabilize the motor angular velocity at this value. If the regulation loop is efficient, the difference between the desired and actual velocities remains small, even when the desired velocity and the motor load vary continuously (at least within a certain range). This type of robustness allows in turn to view the desired velocity as a free control variable. Many controllers supplied with industrial manipulator arms are based on this principle.

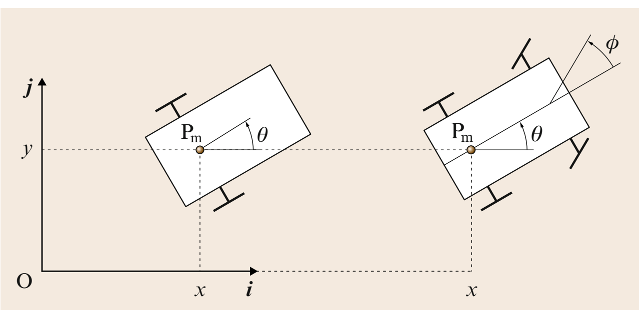

Fig. 34.3 Configuration variables

3. If the servo loops evoked above, whose role is to decouple the kinematics from the dynamics of the vehicle, are not present, one can design them and even improve their performance by using the information that one has of the terms involved in the dynamic equation (34.1). For instance, assume that the torques produced by the actuators can be used as control inputs, a simple way to proceed (at least theoretically) consists in applying the so-called *computed torque* method. The idea is to linearize the dynamic equation by setting

$$\boldsymbol{\tau} = \boldsymbol{\Gamma}(\phi)^{-1}[\boldsymbol{H}(\boldsymbol{q})\boldsymbol{w} + \boldsymbol{F}(\boldsymbol{q}, \boldsymbol{u})\boldsymbol{u}] \,.$$

This yields the simple decoupled linear control system $\dot{\boldsymbol{u}} = \boldsymbol{w}$ with the variable $\boldsymbol{w}$, homogeneous to a vector of accelerations, playing the role of a new control input vector. This latter equation indicates that the problem of controlling the vehicle with motor torques can be brought back to a problem with acceleration control inputs. It is usually not difficult to deduce a control solution to this problem from a velocity control solution devised by using a kinematic model. For instance,

$$\begin{aligned}\boldsymbol{w} &= -k(\boldsymbol{u} - \boldsymbol{u}^*(z, t)) \\ &\quad + \frac{\partial \boldsymbol{u}^*}{\partial z}(z, t)\boldsymbol{B}(z)\boldsymbol{u} + \frac{\partial \boldsymbol{u}^*}{\partial t}(z, t)\end{aligned}$$

with $k > 0$ is a solution if $\boldsymbol{u}^*$ is a differentiable kinematic solution and

$$\boldsymbol{u} = \boldsymbol{u}^*(z, t) + (\boldsymbol{u}(0) - \boldsymbol{u}^*(z_0, 0))\,\mathrm{e}^{-kt}$$

is also a solution.

For the unicycle-type mobile robot, the kinematic model (34.3) used from now on is

$$\begin{cases} \dot{x} = u_1 \cos\theta \,, \\ \dot{y} = u_1 \sin\theta \,, \\ \dot{\theta} = u_2 \,, \end{cases} \tag{34.4}$$

where (x, y) represents the coordinates of the point $\mathrm{P_m}$ located at mid-distance of the actuated wheels, and the angle θ characterizes the robot's chassis orientation (Fig. 34.3). In this equation, u_1 represents the intensity of the vehicle's longitudinal velocity, and u_2 is the chassis instantaneous velocity of rotation. The variables u_1 and u_2 are themselves related to the angular velocity of the actuated wheels via the one-to-one relations

$$u_1 = \frac{r}{2}(\dot{\psi}_\mathrm{r} + \dot{\psi}_\ell)$$

$$u_2 = \frac{r}{2R}(\dot{\psi}_\mathrm{r} - \dot{\psi}_\ell)$$

with r the wheels' radius, R the distance between the two actuated wheels, and $\dot{\psi}_r$ (resp. $\dot{\psi}_\ell$) the angular velocity of the right (resp. left) rear wheel.

For the car-like mobile robot, the kinematic model (34.3) used from now on is

$$\begin{cases} \dot{x} = u_1 \cos\theta \,, \\ \dot{y} = u_1 \sin\theta \,, \\ \dot{\theta} = \frac{u_1}{L} \tan\phi \,, \\ \dot{\phi} = u_2 \,, \end{cases} \tag{34.5}$$

where ϕ represents the vehicle's steering wheel angle, and L is the distance between the rear and front wheels' axles. In all forthcoming simulations, L is set equal to 1.2 m.

34.2.2 Modeling in a Frénet Frame

The object of this subsection is to generalize the previous kinematic equations when the reference frame is a Frénet frame. This generalization will be used later on when addressing the path following problem.

Let us consider a curve $\mathcal{C}$ in the plane of motion, as illustrated on Fig. 34.4, and let us define three frames $\mathcal{F}_0$, $\mathcal{F}_m$, and $\mathcal{F}_s$, as follows. $\mathcal{F}_0 = \{0, \boldsymbol{i}, \boldsymbol{j}\}$ is a fixed frame, $\mathcal{F}_m = \{P_m, \boldsymbol{i}_m, \boldsymbol{j}_m\}$ is a frame attached to the mobile robot with its origin – the point P_m – located on the rear wheels axle, at the mid-distance of the wheels, and $\mathcal{F}_s = \{P_s, \boldsymbol{i}_s, \boldsymbol{j}_s\}$, which is indexed by the curve's curvilinear abscissa s, is such that the unit vector $\boldsymbol{i}_s$ tangents $\mathcal{C}$.

Consider now a point P attached to the robot chassis, and let (l_1, l_2) denote the coordinates of P expressed in the basis of $\mathcal{F}_m$. To determine the equations of motion of P with respect to the curve $\mathcal{C}$ let us introduce three variables s, d, and θ_e, defined as follows.

- s is the curvilinear abscissa at the point P_s obtained by projecting P orthogonally on $\mathcal{C}$. This point exists and is unique if the point P is close enough to the curve. More precisely, it suffices that the distance between P and the curve be smaller than the lower bound of the curve radii. We will assume that this condition is satisfied.
- d is the ordinate of P in the frame $\mathcal{F}_s$; its absolute value is also the distance between P and the curve.
- $\theta_e = \theta - \theta_s$ is the angle characterizing the orientation of the robot chassis with respect to the frame $\mathcal{F}_s$.

Let us now determine $\dot{s}$, $\dot{d}$, and $\dot{\theta}_e$. By definition of the curvature $c(s)$ of $\mathcal{C}$ at P_s, i.e., $c(s) = \partial\theta_s/\partial s$, one deduces from (34.4) that

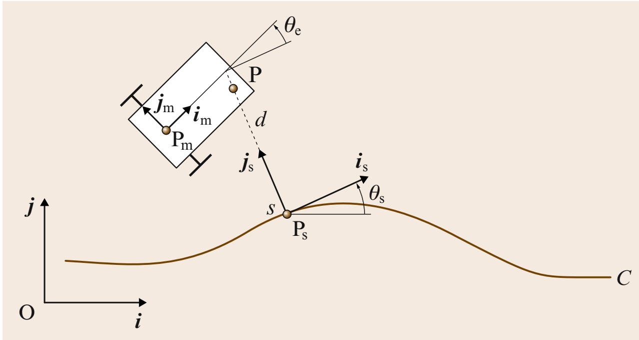

Fig. 34.4 Representation in a Frénet frame

$$\dot{\theta}_e = u_2 - \dot{s}c(s) \,. \tag{34.6}$$

Since $\boldsymbol{P}_s\boldsymbol{P} = d\boldsymbol{j}_s$, by using the equality $\mathrm{d}\boldsymbol{OP}_s/\mathrm{d}t = \dot{s}\boldsymbol{i}_s$ it first emerges that

$$\begin{aligned} \frac{\partial \boldsymbol{OP}}{\partial t} &= \frac{\partial \boldsymbol{OP}_s}{\partial t} + \dot{d}\boldsymbol{j}_s - dc(s)\dot{s}\boldsymbol{i}_s \\ &= \dot{s}(1 - dc(s))\boldsymbol{i}_s + \dot{d}\boldsymbol{j}_s \,. \end{aligned} \tag{34.7}$$

One also has $\boldsymbol{P}_m\boldsymbol{P} = l_1\boldsymbol{i}_m + l_2\boldsymbol{j}_m$. Since $\mathrm{d}\boldsymbol{OP}_m/\mathrm{d}t = u_1\boldsymbol{i}_m$, one gets

$$\begin{aligned} \frac{\partial \boldsymbol{OP}}{\partial t} &= \frac{\partial \boldsymbol{OP}_m}{\partial t} + l_1u_2\boldsymbol{j}_m - l_2u_2\boldsymbol{i}_m \\ &= (u_1 - l_2u_2)\boldsymbol{i}_m + l_1u_2\boldsymbol{j}_m \\ &= (u_1 - l_2u_2)(\cos\theta_e\boldsymbol{i}_s + \sin\theta_e\boldsymbol{j}_s) \\ &\quad + l_1u_2(-\sin\theta_e\boldsymbol{i}_s + \cos\theta_e\boldsymbol{j}_s) \\ &= [(u_1 - l_2u_2)\cos\theta_e - l_1u_2\sin\theta_e]\boldsymbol{i}_s \\ &\quad + [(u_1 - l_2u_2)\sin\theta_e + l_1u_2\cos\theta_e]\boldsymbol{j}_s \,. \end{aligned} \tag{34.8}$$

By forming the scalar products of the vectors in (34.7) and (34.8) with $\boldsymbol{i}_s$ and $\boldsymbol{j}_s$, and by using (34.6), one finally obtains the following system of equations:

$$\begin{cases} \dot{s} = \frac{1}{1-dc(s)}[(u_1 - l_2u_2)\cos\theta_e - l_1u_2\sin\theta_e] \,, \\ \dot{d} = (u_1 - l_2u_2)\sin\theta_e + l_1u_2\cos\theta_e \,, \\ \dot{\theta}_e = u_2 - \dot{s}c(s) \,. \end{cases} \tag{34.9}$$

These equations are a generalization of (34.4). To verify this, it suffices to take P as the origin of the frame $\mathcal{F}_m$ (i.e., $l_1 = l_2 = 0$) and identify the axis $(O, \boldsymbol{i})$ of the frame $\mathcal{F}_0$ with the curve $\mathcal{C}$. Then $s = x$, $c(s) = 0$ $(\forall s)$, and, by setting $y \equiv d$ and $\theta \equiv \theta_e$, one recovers (34.4) exactly.

For car-like vehicles, one easily verifies, by using (34.5), that the system (34.9) becomes

$$\begin{cases} \dot{s} = \frac{u_1}{1-dc(s)}\left[\cos\theta_e - \frac{\tan\phi}{L}(l_2\cos\theta_e + l_1\sin\theta_e)\right] ,\\ \dot{d} = u_1\left[\sin\theta_e + \frac{\tan\phi}{L}(l_1\cos\theta_e - l_2\sin\theta_e)\right] ,\\ \dot{\theta}_e = \frac{u_1}{L}\tan\phi - \dot{s}c(s) ,\\ \dot{\phi} = u_2 , \end{cases} \tag{34.10}$$

(it suffices to replace $u_2 = \dot{\theta}$ in (34.9) by the new value of $\dot{\theta}$: $(u_1 \tan\phi)/L$). To summarize, we have shown the following result.

Proposition 34.1
The kinematic equations of unicycle-type and car-like vehicles, expressed with respect to a Frénet frame, are given by the systems (34.9) and (34.10), respectively.

34.3 Adaptation of Control Methods for Holonomic Systems

We address in this section the problems of trajectory stabilization and path following. When we defined these problems in the introduction, we considered a reference point P attached to the robot chassis. It turns out that the choice of this point is important. Indeed, consider for instance the equations (34.9) for a unicycle point P when $\mathcal{C}$ is the axis $(O, \boldsymbol{i})$. Then, $s = x_P$, $d = y_P$, and $\theta_e = \theta$ represent the robot's posture with respect to the fixed reference frame $\mathcal{F}_0$. There are two possible cases depending on whether P is, or is not, located on the actuated wheels axle. Let us consider the first case, for which $l_1 = 0$. From the first two equations of (34.9), one has

$$\dot{x}_P = (u_1 - l_2u_2)\cos\theta , \quad \dot{y}_P = (u_1 - l_2u_2)\sin\theta .$$

These relations indicate that P can move only in the direction of the vector $(\cos\theta, \sin\theta)$. This is a direct consequence of the nonholonomy constraint to which the vehicle is subjected. Now, if P is not located on the wheels axle, then

$$\begin{pmatrix}\dot{x}_P\\ \dot{y}_P\end{pmatrix} = \begin{pmatrix}\cos\theta & -l_1\sin\theta\\ \sin\theta & l_1\cos\theta\end{pmatrix}\begin{pmatrix}1 & -l_2\\ 0 & 1\end{pmatrix}\begin{pmatrix}u_1\\ u_2\end{pmatrix} . \tag{34.11}$$

The fact that the two square matrices in the right-hand side of this equality are invertible indicates that $\dot{x}_P$ and $\dot{y}_P$ can take any values, and thus that the motion of P is not constrained. By analogy with holonomic manipulator arms, this means that P may be seen as the extremity of a two-degree-of-freedom (2-DOF) manipulator, and thus that it can be controlled by applying the same control laws as those used for manipulators. In this section, we assume that the point P, used to characterize the robot's position, is chosen away from the rear wheels axle. In this case we will see that the problems of trajectory stabilization and path following can be solved very simply. However, as shown in the subsequent section, choosing P on the wheels axle may also be of interest in order to better control the vehicle's orientation.

34.3.1 Stabilization of Trajectories for a Nonconstrained Point

Unicycle

Consider a differentiable reference trajectory $t \longmapsto (x_r(t), y_r(t))$ in the plane. Let $e = (x_P - x_r, y_P - y_r)$ denote the tracking error in position. The control objective is to asymptotically stabilize this error at zero. In view of (34.11), the error equations are

$$\dot{e} = \begin{pmatrix}\cos\theta & -l_1\sin\theta\\ \sin\theta & l_1\cos\theta\end{pmatrix}\begin{pmatrix}u_1 - l_2u_2\\ u_2\end{pmatrix} - \begin{pmatrix}\dot{x}_r\\ \dot{y}_r\end{pmatrix} . \tag{34.12}$$

Introducing new control variables (v_1, v_2) defined by

$$\begin{pmatrix}v_1\\ v_2\end{pmatrix} = \begin{pmatrix}\cos\theta & -l_1\sin\theta\\ \sin\theta & l_1\cos\theta\end{pmatrix}\begin{pmatrix}u_1 - l_2u_2\\ u_2\end{pmatrix} \tag{34.13}$$

the equations (34.12) become simply

$$\dot{e} = \begin{pmatrix}v_1\\ v_2\end{pmatrix} - \begin{pmatrix}\dot{x}_r\\ \dot{y}_r\end{pmatrix} .$$

The classical techniques of stabilization for linear systems can then be used. For instance, one may consider a proportional feedback control with precompensation such as

$$\begin{aligned} v_1 &= \dot{x}_r - k_1e_1 = \dot{x}_r - k_1(x_P - x_r) , \quad (k_1 > 0) ,\\ v_2 &= \dot{y}_r - k_2e_2 = \dot{y}_r - k_2(y_P - y_r) , \quad (k_2 > 0) , \end{aligned}$$

which yields the closed-loop equation $\dot{e} = -Ke$. Of course, this control can be rewritten for the initial control variables $\boldsymbol{u}$, since the mapping $(u_1, u_2) \longmapsto (v_1, v_2)$ is bijective.

Unicycle with Trailers

The previous technique extends directly to the case of a unicycle-type vehicle to which one or several trailers are hooked, provided that the point P is chosen away from the actuated wheels axle and on the side opposite to the trailers. Besides, it is preferable in practice that the robot's longitudinal velocity u_1 remains positive all the time in order to prevent the relative orientations between all vehicles (i. e., the non-actively controlled variables involved in the system's *zero dynamics*) to take overly large values (the jackknife effect). This issue will be discussed further in Sect. 34.4.

Car

This technique also extends to car-like vehicles by choosing a point P attached to the steering wheel frame and not located on the steering wheel axle.

34.3.2 Path Following with No Orientation Control

Unicycle

Let us adopt the notation of Fig. 34.4 to address the problem of following a path associated with a curve $\mathcal{C}$ in the plane. The control objective is to stabilize the distance d at zero. From (34.9), one has

$$\dot{d} = u_1 \sin\theta_e + u_2(-l_2 \sin\theta_e + l_1 \cos\theta_e)\,. \qquad (34.14)$$

Recall that in this case the vehicle's longitudinal velocity u_1 is either imposed or prespecified. We will assume that the product $l_1 u_1$ is positive, i. e., the position of the point P with respect to the actuated wheels axle is chosen in relation to the sign of u_1. This assumption will be removed in Sect. 34.4. To simplify, we will also assume that $l_2 = 0$, i. e., the point P is located on the axis $(P_m, \boldsymbol{i}_m)$. Let us then consider the following feedback control law

$$u_2 = -\frac{u_1}{l_1 \cos\theta_e}\sin\theta_e - \frac{u_1}{\cos\theta_e}k(d,\theta_e)d \qquad (34.15)$$

with k a continuous, strictly positive, function on $\mathbb{R}\times(-\pi/2,\pi/2)$ such that $k(d,\pm\pi/2)=0$. Since $l_2=0$, applying the control (34.15) to (34.14) gives

$$\dot{d} = -l_1 u_1 k(d,\theta_e)d\,.$$

Since $l_1 u_1$ and k are strictly positive, this relation implies that $|d|$ is nonincreasing along any trajectory of the controlled system. For convergence of d to zero, it suffices that

1. the sign of u_1 remains the same,
2. $\pi/2 - |\theta_e(t)| > \epsilon > 0$ for all t, and
3. $$\int_0^t |u_1(s)|\,ds \longrightarrow +\infty \quad \text{when } t \longrightarrow +\infty\,.$$

This latter condition is satisfied, for instance, when u_1 is constant. In this case, d converges to zero exponentially. There just remains to examine the conditions under which u_2, as given by (34.15), is always defined. Since the function in the right-hand side of (34.15) is not defined when $\cos\theta_e = 0$, we are going to determine conditions on the system parameters and the initial state values the satisfaction of which implies that $\cos\theta_e$ cannot approach zero. To this purpose, let us consider the limit value of $\dot\theta_e$ when θ_e tends to $\pi/2$ (resp. $-\pi/2$) from below (resp. from above). By using (34.9), (34.15), and the fact that $l_2 = 0$, a simple calculation shows that

$$\begin{aligned}\dot\theta_e = u_1 \Bigg[&-\frac{c(s)}{1-dc(s)}\cos\theta_e \\ &-\left(1+\frac{l_1 c(s)}{1-dc(s)}\sin\theta_e\right) \\ &\times\left(\frac{\tan\theta_e}{l_1}+\frac{k(d,\theta_e)d}{\cos\theta_e}\right)\Bigg]\,.\end{aligned}$$

Let us assume first that θ_e tends to $\pi/2$ from below. Then the sign of $\dot\theta_e$ is given, in the limit, by the sign of

$$-u_1\left(1+\frac{l_1 c(s)}{1-dc(s)}\right)\frac{1}{l_1}\,.$$

To prevent θ_e from reaching $\pi/2$ it suffices that this sign be negative. It is so if

$$\left|\frac{l_1 c(s)}{1-dc(s)}\right| < 1\,. \qquad (34.16)$$

Now, if θ_e tends to $-\pi/2$ from above, the sign of $\dot\theta_e$ is given, in the limit, by the sign of

$$-u_1\left(1-\frac{l_1 c(s)}{1-dc(s)}\right)\left(\frac{-1}{l_1}\right)\,.$$

To prevent θ_e from reaching $-\pi/2$ it suffices that this sign be positive, and such is the case if (34.16) is true. From this analysis one obtains the following proposition.

Proposition 34.2

Consider the path following problem for a unicycle-type mobile robot with

- [A.] a strictly positive, or strictly negative, longitudinal velocity u_1.
- [B.] a reference point P of coordinates $(l_1, 0)$ in the vehicle's chassis frame, with $l_1 u_1 > 0$.

Let k denote a continuous function, strictly positive on $\mathbb{R} \times (-\pi/2, \pi/2)$, and such that $k(d, \pm\pi/2) = 0$ for every d (for instance, $k(d, \theta_e) = k_0 \cos\theta_e$). Then, for any initial conditions $(s(0), d(0), \theta_e(0))$ such that

$$\theta_e(0) \in \left(-\frac{\pi}{2}, \frac{\pi}{2}\right), \qquad \frac{l_1 c_{max}}{1 - |d(0)| c_{max}} < 1$$

with $c_{max} = \max_s |c(s)|$, the feedback control

$$u_2 = -\frac{u_1 \tan\theta_e}{l_1} - u_1 \frac{k(d, \theta_e) d}{\cos\theta_e}$$

makes the distance $|d|$ between P and the curve nonincreasing, and makes it converge to zero if

$$\int_0^t |u_1(s)| \, ds \longrightarrow +\infty \quad \text{when } t \longrightarrow +\infty .$$

Unicycle with Trailers

The above result applies also to this system, except that u_1 has to be positive in order to avoid jackknife effects which otherwise may (will, if u_1 is kept negative long enough) occur because the orientation angles between the vehicles are not actively monitored.

Car

This control technique thus also applies to this case by considering a point P attached to the steering wheel frame, with u_1 positive.

34.4 Methods Specific to Nonholonomic Systems

The control technique presented in the previous section has the advantage of being simple. However, it is not well suited for all control purposes. One of its main limitations is that it relies on the invariance of the sign of the robot's longitudinal velocity (see the assumptions in Proposition 34.2). For systems with trailers, this velocity is further required to be positive. This condition/restriction is related to the fact that the orientation variables are not actively monitored. To understand its nature better, let us consider the control solution given in Proposition 34.2 for $u_1 > 0$, and assume that this control is applied with u_1 negative (and constant, for instance), with the point P being unchanged. Figure 34.5 illustrates a possible *scenario*. The chosen curve is a simple straight line and we assume that, at time $t = 0$, P is already on this curve (i. e., $d = 0$). If u_1 is negative, while P is bound to stay on the line, the magnitude $|\theta_e|$ of the robot's orientation angle increases rapidly. The angle θ_e reaches $-\pi/2$ at $t = 1$. At this time the control expression is no longer defined (explosion in finite time) and, since the velocity vector has become orthogonal to the curve, the point P can no longer stay on the curve.

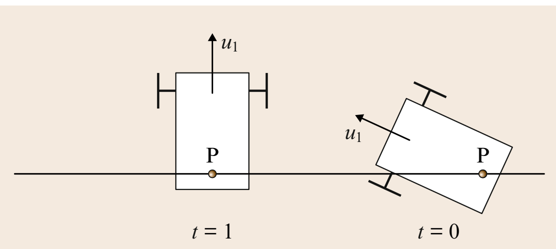

Fig. 34.5 Path-following instability with reverse longitudinal velocity

The explanation for this behavior is as follows. Since the orientation is not controlled, the variable θ_e has its own, a priori unknown, dynamics. It can be stable, or unstable. For the considered control solution, we have shown that it is stable when $u_1 > 0$. In particular, θ_e remains in the domain of definition $(-\pi/2, \pi/2)$ of the feedback law for u_2. When $u_1 < 0$, this dynamics becomes unstable and θ_e reaches the border of the control law's domain of definition $(-\pi/2, \pi/2)$. This instability upon the part of the system which is not directly controlled (the system's *zero dynamics*, in the control terminology) occurs in the same manner when trailers are hooked to a leading vehicle. When the longitudinal velocity is positive, the vehicle has a *pulling* action which tends to align the followers along the curve. In the other case, the leader has a pushing action which tends to misalign them (the jackknife effect). In order to remove this constraint on the sign of the longitudinal velocity, the control has to be designed so that all orientation angles are actively stabilized. An indirect way to do this consists in choosing the point P on the actuated wheels axle, at the mid-distance of the wheels, for instance. In this case, the nonholonomy constraints intervene much more explicitly, and the control can no longer be obtained by applying the techniques used for holonomic manipulators.

This section is organized as follows. First, the modeling equations with respect to a Frénet frame are recast into a canonical form called the chained form. From there, a solution to the path-following problem with active stabilization of the vehicle's orientation is worked out. The problem of (feasible) trajectory stabilization is also revisited with the complementary objective of controlling the vehicle's orientation. The asymptotic stabilization of fixed postures is then addressed. Finally, some comments on the limitations of the proposed control strategies, in relation to the objective of asymptotic stabilization, serve to motivate and introduce a new control approach developed in the subsequent section.

34.4.1 Transformation of Kinematic Models into the Chained Form

In the next chapter dedicated to path planning, it is shown how the kinematic equations of the mobile robots here considered (unicycle-type, car-like, with trailers) can be transformed into the chain form via a change of state and control variables. In particular, the equations of a unicycle (34.4), and those of a car (34.5), can be transformed into a three-dimensional and a four-dimensional chained system, respectively. Those of a unicycle-type vehicle with N trailers yield a chained system of dimension $N+3$ when the trailers are hooked to each other in a specific way. As shown below, this transformation can be generalized to the kinematic models derived with respect to a Frénet frame. The result will be given only for the unicycle and car cases (equations (34.9) and (34.10)), but it also holds when trailers are hooked to such vehicles. The reference point P is now chosen at the mid-distance of the vehicle's rear wheels (or at the mid-distance of the wheels of the last trailer, when trailers are involved).

Let us start with the unicycle case. Under the assumption that P corresponds to the origin of $\mathcal{F}_\mathrm{m}$, one has $l_1 = l_2 = 0$ so that the system (34.9) simplifies to

$$\begin{cases} \dot{s} = \frac{u_1}{1-dc(s)} \cos\theta_\mathrm{e} \;, \\ \dot{d} = u_1 \sin\theta_\mathrm{e} \;, \\ \dot{\theta}_\mathrm{e} = u_2 - \dot{s}c(s) \;. \end{cases} \tag{34.17}$$

Let us determine a change of coordinates and control variables $(s, d, \theta_\mathrm{e}, u_1, u_2) \longmapsto (z_1, z_2, z_3, v_1, v_2)$ allowing to (locally) transform (34.17) into the three-dimensional chained system

$$\begin{cases} \dot{z}_1 = v_1 \;, \\ \dot{z}_2 = v_1 z_3 \;, \\ \dot{z}_3 = v_2 \;. \end{cases} \tag{34.18}$$

By first setting

$$z_1 = s \;, \quad v_1 = \dot{s} = \frac{u_1}{1-dc(s)} \cos\theta_\mathrm{e} \;,$$

we already obtain $\dot{z}_1 = v_1$. This implies that

$$\begin{aligned} \dot{d} &= u_1 \sin\theta_\mathrm{e} = \frac{u_1}{1-dc(s)} \cos\theta_\mathrm{e}[1-dc(s)] \tan\theta_\mathrm{e} \\ &= v_1[1-dc(s)] \tan\theta_\mathrm{e} \;. \end{aligned}$$

We then set $z_2 = d$ et $z_3 = [1-dc(s)]\tan\theta_\mathrm{e}$, so that the above equation becomes $\dot{z}_2 = v_1 z_3$. Finally, we define

$$\begin{aligned} v_2 &= \dot{z}_3 \\ &= [-\dot{d}c(s) - d\frac{\partial c}{\partial s}\dot{s}] \tan\theta_\mathrm{e} \\ &\quad + [1-dc(s)](1+\tan^2\theta_\mathrm{e})\dot{\theta}_\mathrm{e} \;. \end{aligned}$$

The equations (34.18) are satisfied with the variables z_i and v_i so defined.

From this construction it is simple to verify that the mapping $(s, d, \theta_\mathrm{e}) \longmapsto z$ is a *local* change of coordinates defined on $\mathbb{R}^2 \times (-\pi/2, \pi/2)$ (to be more rigorous, one should also take the constraint $|d| < 1/c(s)$ into account). Let us finally remark that the change of control variables involves the derivative $(\partial c/\partial s)$ of the path's curvature (whose knowledge is thus needed for the calculations). One can similarly transform the car's equations into a four-dimensional chained system, although the calculations are slightly more cumbersome. Let us summarize these results in the following proposition.

Proposition 34.3

The change of coordinates and of control variables $(s, d, \theta_\mathrm{e}, u_1, u_2) \longmapsto (z_1, z_2, z_3, v_1, v_2)$ defined by

$$\begin{aligned} (z_1, z_2, z_3) &= (s, d, [1-dc(s)]\tan\theta_\mathrm{e}) \\ (v_1, v_2) &= (\dot{z}_1, \dot{z}_3) \end{aligned}$$

transforms the model (34.17) of a unicycle-type vehicle into a three-dimensional chained system.

Similarly, the change of coordinates and control variables $(s, d, \theta_\mathrm{e}, \phi, u_1, u_2) \longmapsto (z_1, z_2, z_3, z_4, v_1, v_2)$

defined by

$$
\begin{aligned}
(z_1, z_2, z_3, z_4) = \Big\{ & s,\, d,\, [1 - dc(s)] \tan\theta_e, \\
& - c(s)[1 - dc(s)]\big(1 + 2\tan^2\theta_e\big) \\
& - d \frac{\partial c}{\partial s} \tan\theta_e \\
& + [1 - dc(s)]^2 \frac{\tan\phi}{L} \frac{1 + \tan^2\theta_e}{\cos\theta_e} \Big\} , \\
(v_1, v_2) = (\dot{z}_1, \dot{z}_4) &
\end{aligned}
$$

transforms the model (34.10) of a car-like vehicle (with $l_1 = l_2 = 0$) into a four-dimensional chained system.

34.4.2 Tracking of a Reference Vehicle with the Same Kinematics

Let us now consider the problem of tracking, in both position and orientation, a reference vehicle (Fig. 34.6). Contrary to what happens when the control objective is limited to the tracking in position only (Sect. 34.3.1), the choice of the reference point P is of lesser importance because, whatever P, most reference trajectories $t \longmapsto (x_r(t), y_r(t), \theta_r(t))$ are not feasible for the state vector (x_P, y_P, θ). For simplicity, we choose P as the origin P_m of the robot's chassis frame $\mathcal{F}_m$.

Although the terminology is rather loose, the *tracking problem* is usually associated, in the control literature, with the problem of *asymptotically stabilizing* the reference trajectory. In this case, a necessary condition for the existence of a control solution is that the reference is feasible. Feasible trajectories $t \longmapsto (x_r(t), y_r(t), \theta_r(t))$ are smooth time functions which are solution to the robot's kinematic model for some specific control input $t \longmapsto \boldsymbol{u}_r(t) = (u_{1,r}(t), u_{2,r}(t))^\top$, called the *reference control*. For a unicycle-type robot for example, this means in view of (34.4) that

$$
\begin{cases}
\dot{x}_r = u_{1,r} \cos\theta_r \, , \\
\dot{y}_r = u_{1,r} \sin\theta_r \, , \\
\dot{\theta}_r = u_{2,r} \, .
\end{cases} \tag{34.19}
$$

In other words, feasible reference trajectories correspond to the motion of a reference frame $\mathcal{F}_r = \{P_r, \boldsymbol{i}_r, \boldsymbol{j}_r\}$ rigidly attached to a reference unicycle-type robot, with P_r (alike $P = P_m$) located at the mid-distance of the actuated wheels (see Fig. 34.6). From there, the problem is to determine a feedback control which asymptotically stabilizes the tracking error $(x - x_r, y - y_r, \theta - \theta_r)$ at zero, with (x_r, y_r) being the coordinates of P_r in $\mathcal{F}_0$, and θ_r the oriented angles between $\boldsymbol{i}$ and $\boldsymbol{i}_r$. One can proceed as in the path-following case, first by establishing the error equations with respect to the frame $\mathcal{F}_r$, then by transforming these equations in the chain form via a change of variables like the one used to transform the kinematic equations of a mobile robot into a chained system, and finally by designing stabilizing control laws for the transformed system.

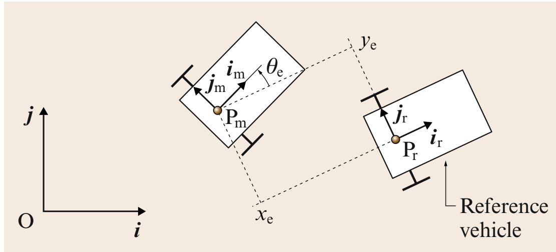

Fig. 34.6 Reference vehicle and error coordinates

Expressing the tracking error in position $(x - x_r, y - y_r)$ with respect to the frame $\mathcal{F}_r$ gives the vector (Fig. 34.6)

$$
\begin{pmatrix} x_e \\ y_e \end{pmatrix} = \begin{pmatrix} \cos\theta_r & \sin\theta_r \\ -\sin\theta_r & \cos\theta_r \end{pmatrix} \begin{pmatrix} x - x_r \\ y - y_r \end{pmatrix} . \tag{34.20}
$$

Calculating the time derivative of this vector yields

$$
\begin{aligned}
\begin{pmatrix} \dot{x}_e \\ \dot{y}_e \end{pmatrix} &= \dot{\theta}_r \begin{pmatrix} -\sin\theta_r & \cos\theta_r \\ -\cos\theta_r & -\sin\theta_r \end{pmatrix} \begin{pmatrix} x - x_r \\ y - y_r \end{pmatrix} \\
&\quad + \begin{pmatrix} \cos\theta_r & \sin\theta_r \\ -\sin\theta_r & \cos\theta_r \end{pmatrix} \begin{pmatrix} \dot{x} - \dot{x}_r \\ \dot{y} - \dot{y}_r \end{pmatrix} \\
&= \begin{pmatrix} u_{2,r} y_e + u_1 \cos(\theta - \theta_r) - u_{1,r} \\ -u_{2,r} x_e + u_1 \sin(\theta - \theta_r) \end{pmatrix} .
\end{aligned}
$$

By denoting $\theta_e = \theta - \theta_r$, the orientation error between the frames $\mathcal{F}_m$ and $\mathcal{F}_r$, we obtain

$$
\begin{cases}
\dot{x}_e = u_{2,r} y_e + u_1 \cos\theta_e - u_{1,r} \, , \\
\dot{y}_e = -u_{2,r} x_e + u_1 \sin\theta_e \, , \\
\dot{\theta}_e = u_2 - u_{2,r} \, .
\end{cases} \tag{34.21}
$$

To determine a control (u_1, u_2) which asymptotically stabilizes the error (x_e, y_e, θ_e) at zero, let us consider the following change of coordinates and control variables

$$
(x_e, y_e, \theta_e, u_1, u_2) \longmapsto (z_1, z_2, z_3, w_1, w_2)
$$

defined by

$$
\begin{aligned}
z_1 &= x_e \,, \\
z_2 &= y_e \,, \\
z_3 &= \tan\theta_e \,, \\
w_1 &= u_1 \cos\theta_e - u_{1,r} \,, \\
w_2 &= \frac{u_2 - u_{2,r}}{\cos^2\theta_e} \,.
\end{aligned}
$$

Note that, around zero, this mapping is only defined when $\theta_e \in (-\pi/2, \pi/2)$. In other words, the orientation error between the physical robot and the reference robot has to be smaller than $\pi/2$.

It is immediate to verify that, in the new variables, the system (34.21) can be written as

$$
\begin{cases}
\dot{z}_1 = u_{2,r} z_2 + w_1 \,, \\
\dot{z}_2 = -u_{2,r} z_1 + u_{1,r} z_3 + w_1 z_3 \,, \\
\dot{z}_3 = w_2 \,.
\end{cases}
\tag{34.22}
$$

We remark that the last term in each of the above three equations corresponds to the one of a chained system. We then have the following result:

Proposition 34.4

The control law

$$
\begin{cases}
w_1 = -k_1 |u_{1,r}| (z_1 + z_2 z_3) \quad (k_1 > 0) \,, \\
w_2 = -k_2 u_{1,r} z_2 - k_3 |u_{1,r}| z_3 \,, \quad (k_2, k_3 > 0) \,,
\end{cases}
\tag{34.23}
$$

renders the origin of the system (34.22) globally asymptotically stable if $u_{1,r}$ is a bounded differentiable function whose derivative is bounded and which does not tend to zero as t tends to infinity.

Remark

By comparison with the results of Sect. 34.3, we note that $u_{1,r}$ may well pass through zero and change its sign.

Proof

Consider the following positive-definite function

$$
V(z) = \frac{1}{2}\left(z_1^2 + z_2^2 + \frac{1}{k_2} z_3^2\right) .
$$

The time derivative of V along the trajectories of the controlled system (34.22–34.23) is given by

$$
\begin{aligned}
\dot{V} &= z_1 w_1 + z_2 (u_{1,r} z_3 + w_1 z_3) + \frac{1}{k_2} z_3 w_2 \\
&= w_1 (z_1 + z_2 z_3) + z_3 \left(u_{1,r} z_2 + \frac{1}{k_2} w_2\right) \\
&= -k_1 |u_{1,r}| (z_1 + z_2 z_3)^2 - \frac{k_3}{k_2} |u_{1,r}| z_3^2 \,.
\end{aligned}
$$

Therefore, along any of these trajectories, V is nonincreasing and converges to some limit value $V_{\lim} \geq 0$. This implies that the variables z_1, z_2, and z_3 are bounded. Since $u_{1,r}$ is continuous, and since its derivative is bounded, $|u_{1,r}|$ is uniformly continuous. Therefore, $\dot{V}$ is uniformly continuous and, by application of Barbalat's lemma, $\dot{V}$ tends to zero when t tends to infinity. In view of the expression of $\dot{V}$, this implies that $u_{1,r} z_3$ and $u_{1,r}(z_1 + z_2 z_3)$ (and thus $u_{1,r} z_1$ also) tend to zero. On the other hand, by using the expression of w_2 ($= \dot{z}_3$) one has

$$
\frac{\mathrm{d}}{\mathrm{d}t}\left(u_{1,r}^2 z_3\right) = 2\dot{u}_{1,r} u_{1,r} z_3 - k_3 u_{1,r}^2 |u_{1,r}| z_3 - k_2 u_{1,r}^3 z_2
$$

and one deduces from what precedes that

$$
\frac{\mathrm{d}}{\mathrm{d}t}\left(u_{1,r}^2 z_3\right) + k_2 u_{1,r}^3 z_2
$$

tends to zero. Since $u_{1,r}^3 z_2$ is uniformly continuous (it is continuous and its derivative is bounded), and since $u_{1,r}^2 z_3$ tends to zero, one deduces by application of a slightly extended version of Barbalat's lemma that $u_{1,r}^3 z_2$ (and thus $u_{1,r} z_2$ also) tends to zero. In view of the expression of V, the convergence of $u_{1,r} z_i (i = 1, 2, 3)$ to zero implies the convergence of $u_{1,r} V$ to zero. Therefore, $u_{1,r} V_{\lim} = 0$, and $V_{\lim} = 0$ by using the assumption that $u_{1,r}$ does not tend to zero.

The linearization of the control (34.23) yields the simpler control

$$
\begin{cases}
w_1 = -k_1 |u_{1,r}| z_1 \,, \\
w_2 = -k_2 u_{1,r} z_2 - k_3 |u_{1,r}| z_3 \,.
\end{cases}
$$

Since $w_1 \approx u_1 - u_{1,r}$ and $w_2 \approx u_2 - u_{2,r}$ near the origin, it is legitimate to wonder if the control

$$
\begin{cases}
u_1 = u_{1,r} - k_1 |u_{1,r}| z_1 \,, \\
u_2 = u_{2,r} - k_2 u_{1,r} z_2 - k_3 |u_{1,r}| z_3 \,.
\end{cases}
$$

can also be used for the system (34.21). In fact, it is not difficult to verify, via a classical pole-placement calculation, that this control asymptotically stabilizes the origin of the linear system which approximates the system (34.21) when $u_{1,r}$ and $u_{2,r}$ are constant, with $u_{1,r} \neq 0$. Therefore, it also *locally* asymptotically stabilizes the origin of the system (34.21) when these conditions on

$u_{1,\mathrm{r}}$ and $u_{2,\mathrm{r}}$ are satisfied. This means also that the tuning of the gains $k_{1,2,3}$ can be performed by using classical linear control techniques applied to the linear approximation of the system (34.21). The control (34.23) is in fact designed so that its tuning for the specific velocities $u_{1,\mathrm{r}}=1$ and $u_{2,\mathrm{r}}=0$ gives good results for all other velocities (except, of course, $u_{1,\mathrm{r}}=0$, for which the linear approximation of the system (34.21) is not controllable and the control vanishes). Indeed, the multiplication of all control gains by $\pm u_{1,\mathrm{r}}$ reduces to normalizing the equations of the controlled system with respect to the longitudinal velocity, so that the transient path followed by the vehicle in the process of catching up with the reference vehicle is independent of the intensity of the longitudinal velocity.

Generalization to a Car-Like Vehicle

The previous method extends to the car case. We provide below the main steps of this extension, and leave to the interested reader the task of verifying the details.

Consider the car's kinematic model (34.5), complemented with the following model of the reference car that one wishes to track

$$\begin{cases} \dot{x}_\mathrm{r} = u_{1,\mathrm{r}}\cos\theta_\mathrm{r}\ , \\ \dot{y}_\mathrm{r} = u_{1,\mathrm{r}}\sin\theta_\mathrm{r}\ , \\ \dot{\theta}_\mathrm{r} = \frac{u_{1,\mathrm{r}}}{L}\tan\phi_\mathrm{r}\ , \\ \dot{\phi}_\mathrm{r} = u_{2,\mathrm{r}}\ . \end{cases} \tag{34.24}$$

We assume that there exists $\delta\in(0,\pi/2)$ such that the steering angle ϕ_r belongs to the interval $[-\delta,\delta]$.

By defining x_e, y_e, and θ_e as in the unicycle case, and by setting $\phi_\mathrm{e}=\phi-\phi_\mathrm{r}$, one easily obtains the following system (to be compared with (34.21))

$$\begin{cases} \dot{x}_\mathrm{e} = (\frac{u_{1,\mathrm{r}}}{L}\tan\phi_\mathrm{r})y_\mathrm{e} + u_1\cos\theta_\mathrm{e} - u_{1,\mathrm{r}}\ , \\ \dot{y}_\mathrm{e} = -(\frac{u_{1,\mathrm{r}}}{L}\tan\phi_\mathrm{r})x_\mathrm{e} + u_1\sin\theta_\mathrm{e}\ , \\ \dot{\theta}_\mathrm{e} = \frac{u_1}{L}\tan\phi - \frac{u_{1,\mathrm{r}}}{L}\tan\phi_\mathrm{r}\ , \\ \dot{\phi}_\mathrm{e} = u_2 - u_{2,\mathrm{r}}\ . \end{cases} \tag{34.25}$$

Introduce the new state variables

$$\begin{cases} z_1 = x_\mathrm{e}\ , \\ z_2 = y_\mathrm{e}\ , \\ z_3 = \tan\theta_\mathrm{e}\ , \\ z_4 = \frac{\tan\phi - \cos\theta_\mathrm{e}\tan\phi_\mathrm{r}}{L\cos^3\theta_\mathrm{e}} + k_2 y_\mathrm{e}\ , (k_2>0)\ . \end{cases}$$

We note that for any $\phi_\mathrm{r}\in(-\pi/2,\pi/2)$, the mapping $(x_\mathrm{e},y_\mathrm{e},\theta_\mathrm{e},\phi)\longmapsto z$ defines a diffeomorphism between $\mathbb{R}^2\times(-\pi/2,\pi/2)^2$ and $\mathbb{R}^4$. Introduce now the new control variables

$$\begin{cases} w_1 = u_1\cos\theta_\mathrm{e} - u_{1,\mathrm{r}}\ , \\ w_2 = \dot{z}_4 = k_2\dot{y}_\mathrm{e} + \left(\frac{3\tan\phi}{\cos\theta_\mathrm{e}} - 2\tan\phi_\mathrm{r}\right)\frac{\sin\theta_\mathrm{e}}{L\cos^3\theta_\mathrm{e}}\dot{\theta}_\mathrm{e} \\ \qquad - \frac{u_{2,\mathrm{r}}}{L\cos^2\phi_\mathrm{r}\cos^2\theta_\mathrm{e}} + \frac{u_2}{L\cos^2\phi\cos^3\theta_\mathrm{e}}\ . \end{cases} \tag{34.26}$$

One shows that $(u_1,u_2)\longmapsto(w_1,w_2)$ defines a change of variables for θ_e, ϕ, and ϕ_r, inside the interval $(-\pi/2,\pi/2)$. These changes of state and control variables transform the system (34.25) into

$$\begin{cases} \dot{z}_1 = (\frac{u_{1,\mathrm{r}}}{L}\tan\phi_\mathrm{r})z_2 + w_1\ , \\ \dot{z}_2 = -(\frac{u_{1,\mathrm{r}}}{L}\tan\phi_\mathrm{r})z_1 + u_{1,\mathrm{r}}z_3 + w_1 z_3\ , \\ \dot{z}_3 = -k_2 u_{1,\mathrm{r}} z_2 + u_{1,\mathrm{r}} z_4 \\ \qquad + w_1\left(z_4 - k_2 z_2 + (1+z_3^2)\frac{\tan\phi_\mathrm{r}}{L}\right)\ , \\ \dot{z}_4 = w_2\ . \end{cases} \tag{34.27}$$

Proposition 34.4 then becomes:

Proposition 34.5

The control law

$$\begin{cases} w_1 = -k_1|u_{1,\mathrm{r}}|\left(z_1 + \frac{z_3}{k_2}\left[z_4 + (1+z_3^2)\frac{\tan\phi_\mathrm{r}}{L}\right]\right)\ , \\ w_2 = -k_3 u_{1,\mathrm{r}} z_3 - k_4|u_{1,\mathrm{r}}|z_4\ , \end{cases} \tag{34.28}$$

with $k_{1,2,3,4}$ denoting positive numbers, renders the origin of the system (34.27) globally asymptotically stable if (i) $u_{1,\mathrm{r}}$ is a bounded differentiable function whose derivative is bounded and which does not tend to zero when t tends to infinity, and (ii) $|\phi_\mathrm{r}|$ is smaller or equal to $\delta<\pi/2$.

As in the case of the unicycle, the gain parameters k_i can be tuned from the controlled system's linearization. More precisely, one can verify from (34.25), (34.26), and (34.28), that in the coordinates $\boldsymbol{\eta}=(x_\mathrm{e},y_\mathrm{e},\theta_\mathrm{e},\phi_\mathrm{e}/L)^\top$, the linearization of the controlled system at the equilibrium $\boldsymbol{\eta}=0$ yields, when $u_\mathrm{r}=(1,0)$, the linear system $\dot{\boldsymbol{\eta}}=\boldsymbol{A}\boldsymbol{\eta}$ with

$$\boldsymbol{A} = \begin{pmatrix} -k_1 & 0 & 0 & 0 \\ 0 & 0 & 1 & 0 \\ 0 & 0 & 0 & 1 \\ 0 & -k_2k_4 & -k_3 & -k_4 \end{pmatrix}$$

The control gains k_i can then be chosen to give desired values to the roots of the corresponding characteristic polynomial $P(\lambda) = (\lambda + k_1)(\lambda^3 + k_4\lambda^2 + k_3\lambda + k_2k_4)$. The nonlinear feedback law (34.28) is designed so that this choice also yields good results when the intensity of $u_{1,r}$ is different from 1 and/or varies arbitrarily, provided that the convergence conditions specified in Proposition 34.5 are satisfied.

The simulation shown on Fig. 34.7 illustrates this control scheme. The gain parameters k_i have been chosen as $(k_1, k_2, k_3, k_4) = (1, 1, 3, 3)$. The initial configuration of the reference vehicle (i.e. at $t = 0$), which is represented in Fig. 34.7a by dashed lines, is $(x_r, y_r, \theta_r)(0) = (0, 0, 0)$. The reference control $\boldsymbol{u}_r$ is defined by (34.29). The initial configuration of the controlled robot, represented in the figure by plain lines, is $(x, y, \theta)(0) = (0, -1.5, 0)$. The configurations at time $t = 10$, 20, and 30, are also represented on the figure. Due to the fast convergence of the tracking error to zero (see the time evolution of the components x_e, y_e, θ_e of the tracking error in Fig. 34.7b), one can basically consider that the configurations of both vehicles coincide after time $t = 10$.

$$u_r(t) = \begin{cases} (1,0)^\top , & \text{if } t \in [0, 10] , \\ (-1, 0.5\cos(2\pi(t-10)/5))^\top , & \\ & \text{if } t \in [10, 20] , \\ (1,0)^\top , & \text{if } t \in [20, 30] . \end{cases} \tag{34.29}$$

34.4.3 Path Following with Orientation Control

We reconsider the path-following problem with the reference point P now located on the actuated wheels axle, at the mid-distance of the wheels. The objective is to synthesize a control law which allows the vehicle to follow the path in a stable manner, independently of the sign of the longitudinal velocity.

Unicycle Case

We have seen in Sect. 34.4.1 how to transform kinematic equations with respect to a Frénet frame into the three-dimensional chained system

$$\begin{cases} \dot{z}_1 = v_1 , \\ \dot{z}_2 = v_1 z_3 , \\ \dot{z}_3 = v_2 . \end{cases} \tag{34.30}$$

Recall that $(z_1, z_2, z_3) = (s, d, (1 - dc(s))\tan\theta_e)$ and that $v_1 = u_1/1 - dc(s)\cos\theta_e$. The objective is to determine a control law which asymptotically stabilizes $(d = 0, \theta_e = 0)$ and also ensures that the constraint on the distance d to the path (i.e., $|dc(s)| < 1$) is satisfied along the trajectories of the controlled system. For the control law, a first possibility consists in considering a proportional feedback like

$$v_2 = -v_1 k_2 z_2 - |v_1| k_3 z_3 , \quad (k_2, k_3 > 0) . \tag{34.31}$$

It is then immediate to verify that the origin of the closed-loop subsystem

$$\begin{cases} \dot{z}_2 = v_1 z_3 , \\ \dot{z}_3 = -v_1 k_2 z_2 - |v_1| k_3 z_3 \end{cases} \tag{34.32}$$

is asymptotically stable when v_1 is constant, either positive or negative. Since u_1 (not v_1) is the intensity of

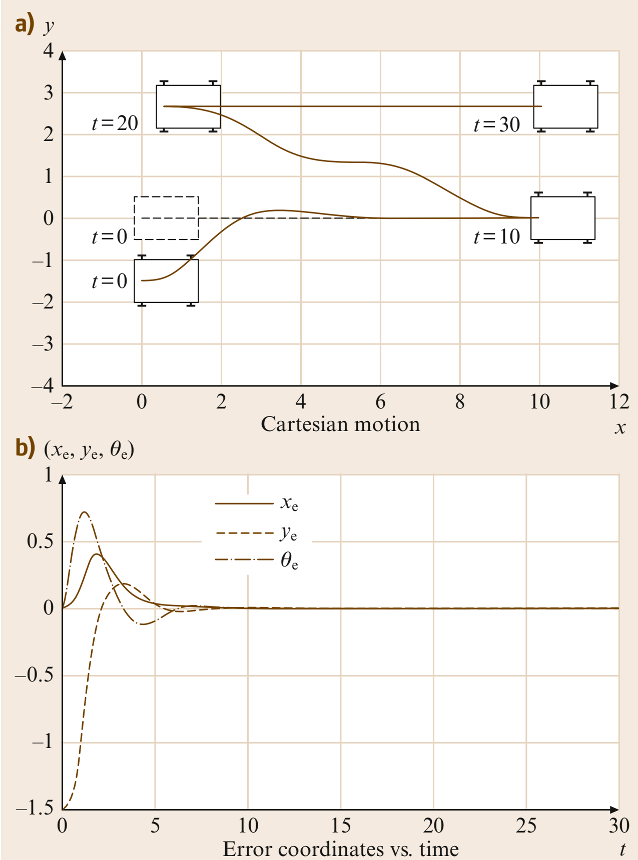

Fig. 34.7a,b Tracking of a reference vehicle

the vehicle's longitudinal velocity, one would rather establish stability conditions which depend on u_1. The following result provides a rather general stability condition and gives a sufficient condition for the satisfaction of the constraint $|dc(s)| < 1$.

Proposition 34.6

Consider the system (34.30) controlled with (34.31), and assume that the initial conditions $[z_2(0), z_3(0)] = [d(0), \{1 - d(0)c[s(0)]\} \tan\theta_e(0)]$ verify

$$z_2^2(0) + \frac{1}{k_2} z_3^2(0) < \frac{1}{c_{\max}^2}$$

with $c_{\max} = \max_s |c(s)|$. Then, the constraint $|dc(s)| < 1$ is satisfied along any solution to the controlled system. Moreover, the function

$$V(z) = \frac{1}{2}\left(z_2^2 + \frac{1}{k_2} z_3^2\right) \tag{34.33}$$

is nonincreasing along any trajectory $z(t)$ of the system, and $V[z(t)]$ tends to zero as t tends to infinity if, for instance, u_1 is a bounded differentiable time function whose derivative is bounded and which does not tend to zero as t tends to infinity.

The proof is similar to the one of Proposition 34.4: a simple calculation shows that the function V is nonincreasing so that, along any solution to the controlled system, it converges to some limit value $V_{\lim}$. The same arguments as those used in the proof of Proposition 34.4 can then be repeated to show that $V_{\lim} = 0$.

Note that the constraints upon u_1 are rather weak. In particular, the sign of u_1 does not have to be constant.

From a practical point of view it can be useful to complement the control action with an integral term. More precisely, let us define a variable z_0 by

$$\dot{z}_0 = v_1 z_2 \,, \quad z_0(0) = 0 \,.$$

The control (34.31) can be modified as follows:

$$\begin{aligned} v_2 &= -|v_1| k_0 z_0 - v_1 k_2 z_2 - |v_1| k_3 z_3 \,, \\ &= -|v_1| k_0 \int_0^t v_1 z_2 - v_1 k_2 z_2 - |v_1| k_3 z_3 \,, \\ &(k_0, k_2, k_3 > 0) \end{aligned} \tag{34.34}$$

and Proposition 34.6 becomes:

Proposition 34.7

Consider the system (34.30) controlled by (34.34) with k_0, k_2, and k_3 such that the polynomial

$$s^3 + k_3 s^2 + k_2 s + k_0$$

is Hurwitz stable (all roots of this polynomial have a negative real part.). Assume also that the initial conditions $[z_2(0), z_3(0)] = [d(0), \{1 - d(0)c[s(0)]\} \tan\theta_e(0)]$ verify:

$$z_2^2(0) + \frac{1}{k_2 - \frac{k_0}{k_3}} z_3^2(0) < \frac{1}{c_{\max}^2} \,.$$

Then the constraint $|dc(s)| < 1$ is satisfied along any solution to the controlled system. Moreover, the function

$$\frac{k_0}{k_3}\left(\int_0^t v_1 z_2\right)^2 + z_2^2(t) + \frac{1}{k_2 - \frac{k_0}{k_3}} z_3^2(t)$$

is nonincreasing along any trajectory of the system, and it tends to zero as t tends to infinity if, for instance, u_1 is a bounded differentiable time-function whose derivative is bounded and which does not converge to zero as t tends to infinity.

Generalization to a Car-Like Vehicle and to a Unicycle-Type Vehicle with Trailers

One of the assets of this type of approach, besides the simplicity of the control law and little demanding conditions of stability associated with it, is that it can be generalized in a straightforward manner to car-like vehicles and unicycle-type vehicles with trailers. The result is summarized in the next proposition by considering a n-dimensional chained system

$$\begin{cases} \dot{z}_1 = v_1 \,, \\ \dot{z}_2 = v_1 z_3 \,, \\ \vdots \\ \dot{z}_{n-1} = v_1 z_n \,, \\ \dot{z}_n = v_2 \,, \end{cases} \tag{34.35}$$

with $n \geq 3$. Its proof is a direct extension of the one in the three-dimensional case. The dimension $n = 4$ corresponds to the car case (Sect. 34.4.1). As for a unicycle-type vehicle with N trailers, one has $n = N + 3$. Recall also that, in all cases, z_2 represents the distance d between the path and the point P located at the mid-distance of the rear wheels of the last vehicle.

Proposition 34.8

Let $k_2, \ldots, k_n$ denote parameters such that the polynomial

$$s^{n-1} + k_n s^{n-2} + k_{n-1} s^{n-3} + \ldots + k_3 s + k_2$$

is Hurwitz stable. With these parameters, let us associate the control law

$$v_2 = -v_1 \sum_{i=2}^{n} \operatorname{sign}(v_1)^{n+1-i} k_i z_i \,. \tag{34.36}$$

Then, there exists a positive-definite matrix $\boldsymbol{Q}$ (whose entries depend on the coefficients k_i) such that, if the initial conditions $[z_2(0), z_3(0), \dots, z_n(0)]$ verify

$$\|[z_2(0), z_3(0), \dots, z_n(0)]\|_Q < \frac{1}{c_{\max}} \tag{34.37}$$

the constraint $|dc(s)| < 1$ is satisfied along any solution to the controlled system. Moreover, the function

$$\|[z_2(t), z_3(t), \dots, z_n(t)]\|_Q$$

is nonincreasing along any trajectory of the system, and it tends to zero as t tends to infinity if, for instance, u_1 is a bounded differentiable function whose derivative is bounded and which does not converge to zero as t tends to infinity.

Remark

The condition (34.37) is always satisfied when $c(s) = 0$ for every s (i. e., when the path is a straight line). It is little demanding in practice when $c_{\max}$ is small. Note also that it is possible to calculate the matrix $\boldsymbol{Q}$ explicitly as a function of the parameters k_i (see [34.1] for more details).

As in the three-dimensional case, it is possible to add an integral term to the control. In this case, the control is calculated from the expression of an *extended system* whose state vector is composed of the variables $z_1, \dots, z_n$, and a complementary variable z_0 such that $\dot{z}_0 = v_1 z_2$. Since adding the variable z_0 preserves the chained structure of the system, the control expression is simply adapted from the one determined for a system of dimension $n+1$ with no integral term. More precisely, one obtains

$$v_2 = -k_0 v_1 \operatorname{sign}(v_1)^n \times \int_0^t v_1 z_2 - v_1 \sum_{i=2}^{n} \operatorname{sign}(v_1)^{n+1-i} k_i z_i$$

with the parameters k_i chosen so that the polynomial $s^n + k_n s^{n-1} + k_{n-1} s^{n-3} + \ldots + k_2 s + k_0$ is Hurwitz stable.

The simulation results reported in Fig. 34.8 illustrate how this control scheme performs for a car-like vehicle. The reference curve is the circle of radius equal to four, centered at the origin. The robot's longitudinal velocity u_1 is defined by $u_1 = 1$ for $t \in [0, 5]$, and $u_1 = -1$ for $t > 5$. The control gains have been chosen as $(k_2, k_3, k_4) = (1, 3, 3)$. The motion of the car-like robot in the plane is represented in Fig. 34.8a, and its configuration at times $t = 0$, 5, and 25 are also depicted in the figure. The time evolution of the variables z_2, z_3, z_4 (defined in Proposition 34.3) is represented in Fig. 34.8b. One can observe that the (discontinuous) change of the longitudinal velocity u_1 at $t = 5$ does not affect the convergence of these variables to zero.

34.4.4 Asymptotic Stabilization of Fixed Postures

We now consider the problem of asymptotic stabilization of a fixed desired (reference) posture (i. e., position

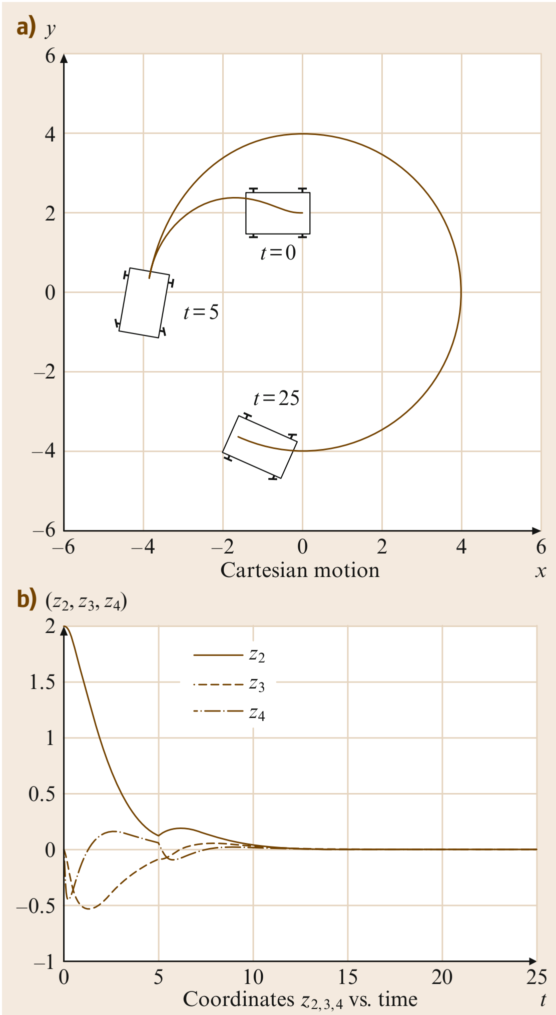

Fig. 34.8a,b Path following along a circle

and orientation) for the robot chassis. This problem may be seen as a limit case of the trajectory tracking problem. However, none of the feedback controllers proposed previously in this chapter provides a solution to this problem. For instance, in Sect. 34.3, although the result about the stabilization in position of feasible trajectories did not exclude the case of a trajectory reduced to a single point, the stability of the vehicle's orientation was not granted in this case. As for the results in Sect. 34.4, the convergence of the posture error to zero has been proven when the robot's longitudinal velocity did not converge to zero (which excludes the case of fixed postures).

From the automatic control point of view, the asymptotic stabilization of fixed postures is very different from the problems of path following and trajectory tracking with nonzero longitudinal velocity, much in the same way as a human driver knows, from experience, that parking a car at a precise location involves techniques and skills different from those exercised when cruising on a road. In particular, it cannot be solved by any classical control method for linear systems (or based on linearization). Technically, the underlying general problem is the one of asymptotic stabilization of equilibria of controllable driftless systems with less control inputs than state variables. This problem motivated numerous studies during the last decade of the last century, from many authors and with various angles of attack, and it has remained a subject of active research five years later. The variety of candidate solutions proposed until now, the mathematical technicalities associated with several of them, together with unsolved difficulties and limitations, particularly (but not only) in terms of robustness (an issue on which we will return), prevent us from attempting to cover the subject exhaustively. Instead, we have opted for a somewhat informal exposition of approaches which have been considered, with the illustration of a few control solutions, without going into technical and mathematical details.

A central aspect of the problem, which triggered much of the subsequent research on the control of nonholonomic systems, is that asymptotic stabilization of equilibria (or fixed points) cannot be achieved by using continuous feedbacks which depend on the state only (i. e., continuous pure-state feedbacks). This is a consequence of an important result due to Brockett in 1983 (see also related comments in Sect. 17.4.2). The original result by Brockett concerned differentiable feedbacks; it has later been extended to the larger set of feedbacks which are only continuous.

Theorem 34.1
(*Brockett* [34.2]) Consider a control system $\dot{x} = f(\boldsymbol{x}, \boldsymbol{u}) \quad (\boldsymbol{x} \in \mathbb{R}^n, \boldsymbol{u} \in \mathbb{R}^m)$, with f a differentiable function and $(\boldsymbol{x}, \boldsymbol{u}) = (0, 0)$ an equilibrium of this system. A necessary condition for the existence of a continuous feedback control $\boldsymbol{u}(\boldsymbol{x})$ which renders the origin of the closed-loop system $\dot{\boldsymbol{x}} = f(\boldsymbol{x}, \boldsymbol{u}(\boldsymbol{x}))$ asymptotically stable is the local surjectivity of the application $(\boldsymbol{x}, \boldsymbol{u}) \longmapsto f(\boldsymbol{x}, \boldsymbol{u})$. More precisely, the image by f of any neighborhood Ω of $(0, 0)$ in $\mathbb{R}^{n+m}$ must be a neighborhood of 0 in $\mathbb{R}^n$.

This result implies that the equilibria of many controllable (nonlinear) systems are not asymptotically stabilizable by continuous pure-state feedbacks. All nonholonomic WMRs belong to this category of systems. This will be shown in the case of a unicycle-type vehicle; the proof for the other mobile robots is similar. Let us thus consider a unicycle-type vehicle, whose kinematic equations (34.4) can be written as $\dot{\boldsymbol{x}} = f(\boldsymbol{x}, \boldsymbol{u})$ with $\boldsymbol{x} = (x_1, x_2, x_3)^\top$, $\boldsymbol{u} = (u_1, u_2)^\top$, and $f(\boldsymbol{x}, \boldsymbol{u}) = (u_1 \cos x_3, u_1 \sin x_3, u_2)^\top$, and let us show that f is not locally onto in the neighborhood of $(\boldsymbol{x}, \boldsymbol{u}) = (0, 0)$. To this purpose, take a vector in $\mathbb{R}^3$ of the form $(0, \delta, 0)^\top$. It is obvious that the equation $f(\boldsymbol{x}, \boldsymbol{u}) = (0, \delta, 0)^\top$ does not have a solution in the neighborhood of $(\boldsymbol{x}, \boldsymbol{u}) = (0, 0)$ since the first equation, namely $u_1 \cos x_3 = 0$, implies that $u_1 = 0$, so that the second equation cannot have a solution if δ is different from zero.

It is also obvious that the linear approximation (about the equilibrium $(\boldsymbol{x}, \boldsymbol{u}) = (0, 0)$) of the unicycle kinematic equations is not controllable. If it were, it would be possible to (locally) asymptotically stabilize this equilibrium with a linear (thus continuous) state feedback.

Therefore, by application of the above theorem, a unicycle-type mobile robot (like other nonholonomic robots) cannot be asymptotically stabilized at a desired posture (position/orientation) by using a continuous pure-state feedback. This impossibility has motivated the development of other control strategies in order to solve the problem. Three major types of controls have been considered:

1. *continuous time-varying feedbacks*, which, besides from depending on the state x, depend also on the exogenous time variable (i. e., $\boldsymbol{u}(\boldsymbol{x}, t)$ instead of $\boldsymbol{u}(\boldsymbol{x})$ for classical feedbacks),
2. *discontinuous feedbacks*, in the classical form $\boldsymbol{u}(\boldsymbol{x})$, except that the function $\boldsymbol{u}$ is not continuous at the equilibrium that one wishes to stabilize,

3. *hybrid discrete/continuous feedbacks*. Although this class of feedbacks is not defined as precisely as the other two sets of controls, it is mostly composed of time-varying feedbacks, either continuous or discontinuous, such that the part of the control which depends upon the state is only updated periodically, e.g., $\boldsymbol{u}(t) = \bar{\boldsymbol{u}}[\boldsymbol{x}(kT), t]$ for any $t \in [kT, (k+1)T]$, with T denoting a constant period, and $k \in \mathbb{N}$.

We will now illustrate these approaches. In fact, only time-varying and hybrid feedbacks will be considered here. The main reason is that discontinuous feedbacks involve difficult questions (existence of solutions, mathematical meaning of these solutions, etc.) which complicate their analysis and for which complete answers are not available. Moreover, for most of the discontinuous control strategies described in the literature, the property of stability in the sense of Lyapunov is either not granted or remains an open issue.

Time-Varying Feedbacks

The use of time-varying feedbacks for the asymptotic stabilization of a fixed desired equilibrium, for a nonholonomic WMR, in order to circumvent the obstruction pointed out by Brockett's Theorem, was first proposed in [34.3]. Since then, very general results about the stabilization of nonlinear systems by means of time-varying feedbacks have been obtained. For instance, it has been proved that any controllable driftless system can have any of its equilibria asymptotically stabilized with a control of this type [34.4]. This includes the kinematic models of the nonholonomic mobile robots here considered. We will illustrate this approach in the case of unicycle-type and car-like mobile robots modeled by three- and four-dimensional chained systems, respectively. In order to consider the three-dimensional case, let us come back on the results obtained in Sect. 34.4.3 for path following. We have established (Proposition 34.6) that the control $v_2 = -v_1 k_2 z_2 - |v_1| k_3 z_3$ applied to the system

$$\begin{cases} \dot{z}_1 = v_1 \,, \\ \dot{z}_2 = v_1 z_3 \,, \\ \dot{z}_3 = v_2 \,, \end{cases}$$

renders the function $V(z)$ defined by (34.33) nonincreasing along any trajectory of the controlled system, i. e.,

$$\dot{V} = -\frac{k_3}{k_2} |v_1| z_3^2 \,,$$

and ensures the convergence of z_2 and z_3 to zero if, for instance, v_1 does not tend to zero as t tends to infinity. For example, if $v_1(t) = \sin t$, the proposition applies, z_2 and z_3 tend to zero, and

$$\begin{aligned} z_1(t) &= z_1(0) + \int_0^t v_1(s)\,\mathrm{d}s = z_1(0) + \int_0^t \sin s\,\mathrm{d}s \\ &= z_1(0) + 1 - \cos t \end{aligned}$$

so that $z_1(t)$ oscillates around the mean value $z_1(0)+1$. To reduce these oscillations, one can multiply v_1 by a factor which depends on the current state. Take, for example, $v_1(z,t) = \|(z_2, z_3)\| \sin t$, that we complement with a stabilizing term like $-k_1 z_1$ with $k_1 > 0$, i. e.,

$$v_1(z,t) = -k_1 z_1 + \|(z_2, z_3)\| \sin t \,.$$

The feedback control so obtained is time-varying and asymptotically stabilizing.

Proposition 34.9
The continuous time-varying feedback

$$\begin{cases} v_1(z,t) = -k_1 z_1 + \alpha \|(z_2, z_3)\| \sin t \,, \\ v_2(z,t) = -v_1(z,t) k_2 z_2 - |v_1(z,t)| k_3 z_3 \,, \end{cases} \tag{34.38}$$

with $\alpha, k_{1,2,3} > 0$, renders the origin of the three-dimensional chained system globally asymptotically stable [34.5].

The above proposition can be extended to chained systems of arbitrary dimension [34.5]. For the case $n = 4$, which corresponds to the car-like robot, one has the following result.

Proposition 34.10
The continuous time-varying feedback

$$\begin{cases} v_1(z,t) = -k_1 z_1 + \alpha \|(z_2, z_3, z_4)\| \sin t \,, \\ v_2(z,t) = -|v_1(z,t)| k_2 z_2 - v_1(z,t) k_3 z_3 \\ \qquad\qquad - |v_1(z,t)| k_4 z_4 \,, \end{cases} \tag{34.39}$$

with $\alpha, k_{1,2,3,4} > 0$ chosen such that the polynomial $s^3 + k_4 s^2 + k_3 s + k_2$ is Hurwitz-stable, renders the origin of the four-dimensional chained system globally asymptotically stable [34.5].

Figure 34.9 below illustrates the previous result. For this simulation, the parameters $\alpha, k_{1,2,3,4}$ in the feedback law (34.39) have been chosen as $\alpha = 3$ and $k_{1,2,3,4} = (1.2, 10, 18, 17)$. Figure 34.9a shows the motion of the

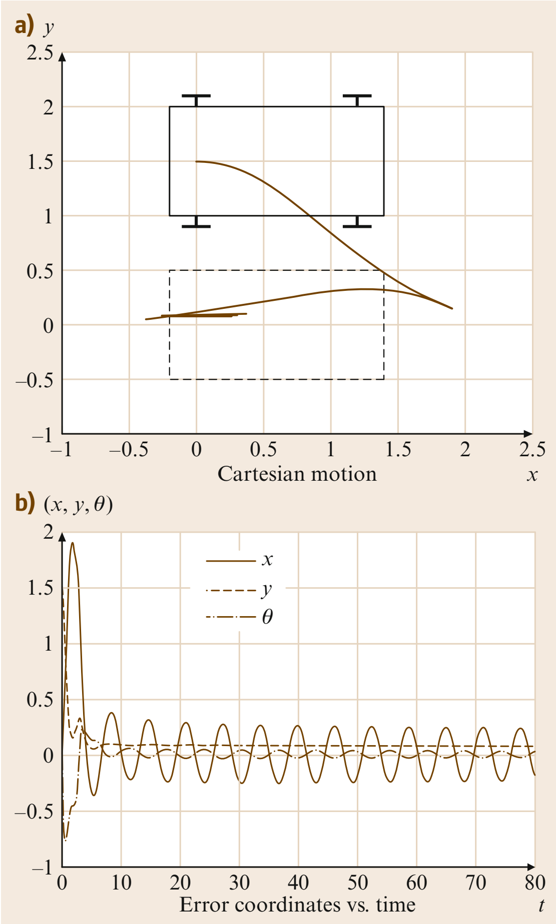

Fig. 34.9a,b Asymptotic stabilization with a Lipschitz-continuous controller

car-like robot in the plane. The initial configuration, at time $t = 0$, is depicted in plain lines, whereas the desired configuration is shown in dashed lines. The time evolution of the variables x, y, and θ (i. e., the position and orientation variables corresponding to the model (34.5)) is shown in Fig. 34.9b.

A shortcoming of this type of control, very clear from this simulation, is that the system's state converges to zero quite slowly. One can show that the rate of convergence is only polynomial, i. e., it is commensurable with $t^{-\alpha}$ (for some $\alpha \in (0, 1)$) for most of the trajectories of the controlled system. This slow rate of convergence is related to the fact that the control function is Lipschitz-continuous with respect to x. It is a characteristics of systems the linear approximation of which is not stabilizable, as specified in the following proposition.

Proposition 34.11

Consider the control system $\dot{\boldsymbol{x}} = f(\boldsymbol{x}, \boldsymbol{u})$ ($\boldsymbol{x} \in \mathbb{R}^n$, $\boldsymbol{u} \in \mathbb{R}^m$) with f being differentiable, and $(\boldsymbol{x}, \boldsymbol{u}) = (0, 0)$ an equilibrium point of this system. Assume that the linear approximation of this system is not stabilizable. Consider also a continuous time-varying feedback $\boldsymbol{u}(\boldsymbol{x}, t)$, periodic with respect to t, such that $\boldsymbol{u}(0, t) = 0$ for any t, and such that $\boldsymbol{u}(., t)$ is $k(t)$-Lipschitz continuous with respect to $\boldsymbol{x}$, for some bounded function k. This feedback cannot yield uniform exponential convergence to zero of the closed-loop system's solutions: there do not exist constants $K > 0$ and $\gamma > 0$ such that, along any trajectory $\boldsymbol{x}(.)$ of the controlled system, one has

$$|x(t)| \leq K|x(t_0)|\,\mathrm{e}^{-\gamma(t-t_0)} . \tag{34.40}$$

The intuitive reason behind this impossibility can easily be illustrated on the unicycle example. When using the chain form representation, the second equation is $\dot{z}_2 = v_1 z_3$. Since the linearization around $(z = 0, v = 0)$ of this equation gives $\dot{z}_2 = 0$, the linear approximation of the system is not controllable (nor stabilizable). In these conditions, exponential convergence, when applying a linear feedback, would necessitate the use of gains growing to infinity, thus ruling out the property of Lipschitz-continuity. This type of reasoning, coupled to the need of better performance and efficiency, has triggered the development of stabilizing time-varying feedbacks which are continuous, but not Lipschitz-continuous. Examples of such feedbacks, yielding uniform exponential convergence, are given in the following propositions for chained systems of dimension three and four, respectively.

Proposition 34.12

Let $\alpha, k_{1,2,3} > 0$ denote scalars such that the polynomial $p(s) = s^2 + k_3 s + k_2$ is Hurwitz stable. For any integers $p, q \in \mathbb{N}^*$, let $\rho_{p,q}$ denote the function defined on $\mathbb{R}^2$ by

$$\forall \bar{z}_2 = (z_2, z_3) \in \mathbb{R}^2,\ \rho_{p,q}(\bar{z}_2) = \left(|z_2|^{\frac{p}{q+1}} + |z_3|^{\frac{p}{q}}\right)^{\frac{1}{p}} .$$

Then, there exists $q_0 > 1$ such that, for any $q \geq q_0$ and $p > q + 2$, the continuous state feedback

$$\begin{cases} v_1(z, t) = -k_1(z_1 \sin t - |z_1|) \sin t \\ \qquad\qquad + \alpha \rho_{p,q}(\bar{z}_2) \sin t \\ v_2(z, t) = -v_1(z, t) k_2 \frac{z_2}{\rho^2_{p,q}(\bar{z}_2)} - |v_1(z, t)| k_3 \frac{z_3}{\rho_{p,q}(\bar{z}_2)} \end{cases} \tag{34.41}$$

renders the origin of the three-dimensional chained system globally asymptotically stable, with a uniform exponential rate of convergence [34.1].

The parenthood of the controls (34.38) and (34.41) is noticeable. One can also verify that the control (34.41) is well defined (by continuity) at $\bar{z}_2 = 0$. More precisely, the ratios

$$\frac{z_2}{\rho^2_{p,q}(\bar{z}_2)} \quad \text{and} \quad \frac{z_3}{\rho_{p,q}(\bar{z}_2)} ,$$

which are obviously well defined when $\bar{z}_2 \neq 0$, tend to zero when $\bar{z}_2$ tends to zero. This guarantees the continuity of the control law.

The property of exponential convergence pointed out in the above result calls for some remarks. Indeed, this property does not exactly correspond to the classical exponential convergence property associated with stable linear systems. In this latter case, exponential convergence implies that the relation (34.40) is satisfied. This corresponds to the common notion of *exponential stability*. In the present case, this inequality becomes

$$\rho[z(t)] \leq K\rho[z(t_0)]\,\mathrm{e}^{-\gamma(t-t_0)}$$

for some function ρ, defined for example by $\rho(z) = |z_1| + \rho_{p,q}(z_2, z_3)$, with $\rho_{p,q}$ as specified in Proposition 34.12. Although the function ρ shares common features with the Euclidean norm of the state vector (it is definite positive and it tends to infinity when $\|z\|$ tends to infinity), it is not equivalent to this norm. Of course, this does not change the fact that each component z_i of z converges to zero exponentially. However, the transient behavior is different because one only has

$$|z_i(t)| \leq K\|z(t_0)\|^{\alpha}\,\mathrm{e}^{-\gamma(t-t_0)}$$

with $\alpha < 1$, instead of

$$|z_i(t)| \leq K\|z(t_0)\|\,\mathrm{e}^{-\gamma(t-t_0)} .$$

In the case of the four-dimensional chained system, one can establish the following result, which is similar to Proposition 34.12.

Proposition 34.13

Let $\alpha, k_1, k_2, k_3, k_4 > 0$ be chosen such that the polynomial $p(s) = s^3 + k_4 s^2 + k_3 s + k_2$ is Hurwitz stable. For any integers $p, q \in \mathbb{N}^*$, let $\rho_{p,q}$ denote the function defined on $\mathbb{R}^3$ by

$$\rho_{p,q}(\bar{z}_2) = \left(|z_2|^{\frac{p}{q+2}} + |z_3|^{\frac{p}{q+1}} + |z_4|^{\frac{p}{q}}\right)^{\frac{1}{p}}$$

with $\bar{z}_2 = (z_2, z_3, z_4) \in \mathbb{R}^3$. Then, there exists $q_0 > 1$ such that, for any $q \geq q_0$ and $p > q + 2$, the continuous state feedback

$$\begin{cases} v_1(z,t) = -k_1(z_1 \sin t - |z_1|)\sin t \\ \qquad\qquad + \alpha\rho_{p,q}(\bar{z}_2)\sin t\,, \\ v_2(z,t) = -|v_1(z,t)|k_2 \frac{z_2}{\rho^3_{p,q}(\bar{z}_2)} - v_1(z,t)k_3\frac{z_3}{\rho^2_{p,q}(\bar{z}_2)} \\ \qquad\qquad - |v_1(z,t)|k_4\frac{z_4}{\rho_{p,q}(\bar{z}_2)}\,, \end{cases} \tag{34.42}$$

renders the origin of the four-dimensional chained system globally asymptotically stable, with a uniform exponential rate of convergence [34.1].

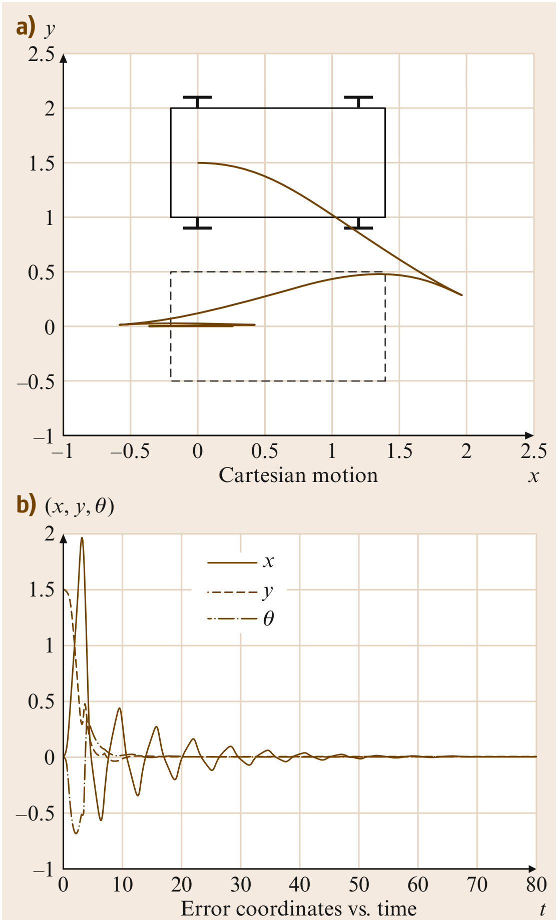

Fig. 34.10a,b Asymptotic stabilization with a continuous (non-Lipschitz) time-varying feedback

The performance of the control law (34.42) is illustrated by the simulation results shown in Fig. 34.10. The control parameters have been chosen as follows: $\alpha = 0.6$, $k_{1,2,3,4} = (1.6, 10, 18, 17)$, $q = 2$, $p = 5$. The comparison with the simulation results of Fig. 34.9 shows a clear gain in performance.

Hybrid Feedbacks

These feedbacks constitute an alternative for the asymptotic stabilization of fixed postures. They may be seen as a mix of open-loop and feedback controls in the sense that the dependence on the state is, in general, only updated periodically (by contrast with time-varying feedbacks which are updated continuously). Between two updates, the control works in open-loop mode. Nonetheless, this type of control may present some advantages with respect to time-varying feedbacks. This point is briefly commented upon a little further. An example of a hybrid feedback is provided in the following proposition.

Proposition 34.14

The hybrid feedback law v defined by

$$v(t) = \bar{v}[z(kT), t] , \quad \forall t \in [kT, (k+1)T] , \quad (34.43)$$

with

$$\begin{cases} \bar{v}_1(z, t) = \frac{1}{T}[(k_1 - 1)z_1 + 2\pi\rho(z)\sin(\omega t)] , \\ \bar{v}_2(z, t) = \frac{1}{T}[(k_3 - 1)z_3 + 2(k_2 - 1)\frac{z_2}{\rho(z)}\cos(\omega t)] , \end{cases}$$

and

$$k_{1,2,3} \in (-1, 1) , \quad \omega = \frac{2\pi}{T} ,$$
$$\rho(z) = \alpha_2 |z_2|^{1/2} , \quad (\alpha_2 > 0)$$

is a $\mathcal{K}(T)$-exponential stabilizer for the three-dimensional chained system [34.6].

The property of $\mathcal{K}(T)$-*exponential stabilizer* evoked in the above proposition means that there exist positive constants K, η, and γ, with $\gamma < 1$, such that for any z_0, the solution at time t of the controlled system associated with the initial condition z_0 at time $t = 0$, which we denote as $z(t, 0, z_0)$, satisfies for any $k \in \mathbb{N}$ and any $s \in [0, T)$ the inequalities

$$\|z((k+1)T, 0, z_0)\| \leq \gamma \|z(kT, 0, z_0)\|$$

and

$$\|z(kT + s, 0, z_0)\| \leq K \|z(kT, 0, z_0)\|^{\eta} .$$

These relations imply the exponential convergence of the system's trajectories to the origin $z = 0$. They do not imply the stability of this point because $\|z(t, 0, z_0)\|$ may vanish at some time $t = \bar{t}$ and not remain equal to zero thereafter. Note, however, that if $\|z(kT, 0, z_0)\| = 0$ for some $k \in \mathbb{N}$, then the above relations imply that $\|z(t, 0, z_0)\| = 0$ for all $t \geq kT$.

In the case of four-dimensional systems, a result similar to Proposition 34.14 can also be established.

Proposition 34.15

The hybrid feedback law v defined by

$$\boldsymbol{v}(t) = \bar{\boldsymbol{v}}(\boldsymbol{z}(kT), t) , \quad \forall t \in [kT, (k+1)T] \quad (34.44)$$

with

$$\begin{cases} \bar{v}_1(z, t) = \frac{1}{T}[(k_1 - 1)z_1 + 2\pi\rho(z)\sin(\omega t)] , \\ \bar{v}_2(z, t) = \frac{1}{T}[(k_4 - 1)z_4 + 2(k_3 - 1)\frac{z_3}{\rho(z)}\cos(\omega t) \\ \qquad + 8(k_2 - 1)\frac{z_2}{\rho^2(z)}\cos(2\omega t)] , \end{cases}$$

$k_{1,2,3,4} \in (-1, 1)$, $\omega = \frac{2\pi}{T}$, and $\rho(z) = \alpha_2 |z_2|^{1/4} + \alpha_3 |z_3|^{1/3}$ $(\alpha_{2,3} > 0)$, is a $\mathcal{K}(T)$-exponential stabilizer for the four-dimensional chained system [34.6].

The simulation results reported in Fig. 34.11 illustrate the application of the feedback law (34.44). The control parameters have been chosen as $T = 3$, $k_{1,2,3,4} = 0.25$, and $\alpha_{2,3} = 0.95$. The control performance is similar to the one observed in Fig. 34.10, as could be expected from the fact that both controls yield exponential convergence to the origin.

34.4.5 Limitations Inherent to the Control of Nonholonomic Systems

Let us first mention some problems associated with the nonlinear time-varying and hybrid feedbacks just presented. An ever important issue, when studying feedback control, is robustness. Indeed, if it were not for the sake of robustness, feedback control would lose much of its value and interest with respect to open-loop control solutions. There are various robustness issues. One of them concerns the sensitivity to modeling errors. For instance, in the case of a unicycle-type robot whose kinematic equations are in the form $\dot{\boldsymbol{x}} = u_1 b_1(\boldsymbol{x}) + u_2 b_2(\boldsymbol{x})$, one would like to know whether a feedback law which stabilizes an equilibrium of this system also stabilizes this equilibrium for the *neighbor* system $\dot{\boldsymbol{x}} = u_1[b_1(\boldsymbol{x}) + \varepsilon g_1(\boldsymbol{x})] + u_2[b_2(\boldsymbol{x}) + \varepsilon g_2(\boldsymbol{x})]$, with g_1 and g_2 denoting continuous applications, and ε a parameter which quantifies the modeling error. This type of error can account,

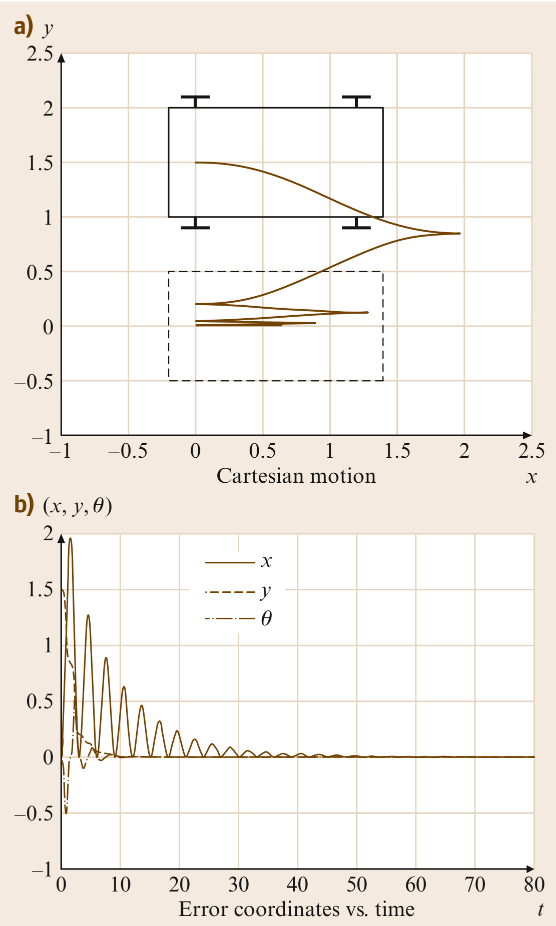

Fig. 34.11a,b Asymptotic stabilization with a hybrid discrete/continuous controller

for example, for a small uncertainty concerning the orientation of the actuated wheels axle with respect to the chassis, which results in a bias in the measurement of this orientation. One can show that time-varying control laws like (34.41) are not robust with respect to this type of error in the sense that, for certain functions g_1 and g_2, and for ε arbitrarily small, the system's solutions end up oscillating in the neighborhood of the origin, instead of converging to the origin. In other words, both the properties of stability of the origin and of convergence to this point can be jeopardized by arbitrarily small modeling errors, even in the absence of measurement noise. In this respect, the hybrid control law (34.43) is more robust: the exponential convergence to the origin of the controlled system's solutions is still obtained when ε is small enough. However, the slightest discretization uncertainty can produce the same type of local instability. In view of these problems, one is brought to question the existence of fast (exponential) stabilizers endowed with robustness properties similar to those of stabilizing linear feedbacks for linear systems. The answer is that, to our knowledge, no such control solution (either continuous or discontinuous) has ever been found. More than likely such a solution does not exist for nonholonomic systems. Robustness of the stability property against modeling errors, and control discretization and delays, has been proved in some cases, but this could only be achieved with Lipschitz-continuous feedbacks which, as we have seen, yield slow convergence. The classical compromise between robustness and performance thus seems much more acute than in the case of stabilizable linear systems (or nonlinear systems whose linear approximation is stabilizable).

A second issue is the proven nonexistence of a *universal* feedback controller capable of stabilizing any feasible reference state trajectory asymptotically [34.7]. This is another notable difference with the linear case. Indeed, given a controllable linear system $\dot{\boldsymbol{x}} = \boldsymbol{A}\boldsymbol{x} + \boldsymbol{B}\boldsymbol{u}$, the feedback controller $\boldsymbol{u} = \boldsymbol{u}_r + \boldsymbol{K}(\boldsymbol{x} - x_r)$, with $\boldsymbol{K}$ a gain matrix such that $\boldsymbol{A} + \boldsymbol{B}\boldsymbol{K}$ is Hurwitz stable, exponentially stabilizes any feasible reference trajectory $\boldsymbol{x}_r$ (solution to the system) associated with the control input $\boldsymbol{u}_r$. The nonexistence of such a controller, in the case of nonholonomic mobile robots, is related to the conditions upon the longitudinal velocity stated in previous propositions concerning trajectory stabilization (Propositions 34.4 and 34.5). This basically indicates that such conditions cannot be removed entirely: whatever the chosen feedback controller, there always exists a feasible reference trajectory that this feedback cannot asymptotically stabilize. Note that this limitation persists when considering nonstandard feedbacks (such as, e.g., time-varying periodic feedbacks capable of asymptotically stabilizing reference trajectories which are reduced to a single point). Moreover, it has clear practical consequences because there are applications (automatic tracking of a human-driven car, for instance) for which the reference trajectory, and thus its properties, are not known in advance (is the leading car going to keep moving or stop?) so that one cannot easily decide on which controller to use. Switching between various controllers is a possible strategy, which has been studied by some authors and may give satisfactory results in many situations. However, since implementing a predefined switching strategy between two controllers sums up to designing a third controller, this does not solve the core of the problem nor grant any certitude of success.

A third issue, which is not specific to nonholonomic systems, but has seldom been addressed in the nonlinear control literature, concerns the problem of tracking *nonfeasible* trajectories (i. e., trajectories which are not solutions to the system's equations). Since exact tracking is not possible, by the definition of a nonfeasible trajectory, the control objective is then to ensure that the tracking errors shrink to, and ever after never exceed, certain nonzero thresholds. The fact that these thresholds can theoretically be arbitrarily small in the case of nonholonomic systems, if the amplitude of the velocity control inputs is not limited, makes this problem particularly relevant for these systems. This can be termed as a *practical* stabilization objective which, although slightly less ambitious than the objective of asymptotic stabilization considered in previous sections, opens up both the control design problem and the range of applications significantly. For instance, it allows to address the problem of tracking an omnidirectional vehicle with a unicycle-type, or a car-like, vehicle. In the context of planning a trajectory with obstacle avoidance, transforming a nonfeasible trajectory into a feasible approximation for a certain mobile robot can be performed by applying a practical stabilizer to a model of this robot and by numerical integration of the system's closed-loop equations. Also, if one reformulates the former question about the existence of a *universal* stabilizer, with the objective of asymptotic stabilization now replaced by the one of practical stabilization, then the answer becomes positive: such a stabilizer exists and, moreover, the reference trajectories do not even have to be feasible.

34.4.6 Practical Stabilization of Arbitrary Trajectories Based on the Transverse Function Approach

A possible approach for the design of practical stabilizers in the case of controllable driftless systems is described in [34.8]. Some of its basic principles, here adapted to the specific examples of unicycle-type and car-like mobile robots, are recalled next.

Let us introduce some matrix notation that will be used in this section.

$$\boldsymbol{R}(\theta) = \begin{pmatrix} \cos\theta & -\sin\theta \\ \sin\theta & \cos\theta \end{pmatrix}, \quad \boldsymbol{S} = \begin{pmatrix} 0 & -1 \\ 1 & 0 \end{pmatrix}$$

$$\bar{\boldsymbol{R}}(\theta) = \begin{pmatrix} R(\theta) & 0 \\ 0 & 1 \end{pmatrix}.$$

Unicycle Case

With the above notation, the kinematic model (34.4) can be written as

$$\dot{\boldsymbol{g}} = \bar{\boldsymbol{R}}(\theta)\boldsymbol{C}\boldsymbol{u} \tag{34.45}$$

with $\boldsymbol{g} = (\boldsymbol{x}, \boldsymbol{y}, \theta)'$ and

$$\boldsymbol{C} = \begin{pmatrix} 1 & 0 \\ 0 & 0 \\ 0 & 1 \end{pmatrix}.$$

Let us now consider a smooth function

$$f : \alpha \longmapsto f(\alpha) = \begin{pmatrix} f_x(\alpha) \\ f_y(\alpha) \\ f_\theta(\alpha) \end{pmatrix}$$

with $\alpha \in S^1 = \mathbb{R}/2\pi\mathbb{Z}$ (i. e., α is an angle variable), and define

$$\begin{aligned} \bar{\boldsymbol{g}} &:= \begin{pmatrix} \bar{\boldsymbol{x}} \\ \bar{\boldsymbol{y}} \\ \bar{\theta} \end{pmatrix} := \boldsymbol{g} - \bar{\boldsymbol{R}}\big(\theta - f_\theta(\alpha)\big) f(\alpha) \\ &= \begin{pmatrix} \begin{pmatrix} x \\ y \end{pmatrix} - \boldsymbol{R}(\theta - f_\theta(\alpha)) \begin{pmatrix} f_x(\alpha) \\ f_y(\alpha) \end{pmatrix} \\ \theta - f_\theta(\alpha) \end{pmatrix}. \end{aligned} \tag{34.46}$$

Note that $\bar{\boldsymbol{g}}$ can be viewed as the situation of a frame $\bar{\mathcal{F}}_{\mathrm{m}}(\alpha)$ the origin of which has components

$$-\boldsymbol{R}(-f_\theta(\alpha)) \begin{pmatrix} f_x(\alpha) \\ f_y(\alpha) \end{pmatrix}$$

in the frame $\mathcal{F}_{\mathrm{m}}$. In term of differential geometry, $\bar{g}$ is the product of g by the inverse $f(\alpha)^{-1}$ of $f(\alpha)$, in the sense of the Lie group operations in $SE(2)$. Hence, $\bar{\mathcal{F}}_{\mathrm{m}}(\alpha)$ is all the closer to $\mathcal{F}_{\mathrm{m}}$ as the components of $f(\alpha)$ are small. For any smooth time function $t \longmapsto \alpha(t)$, and along any solution to system (34.45), the time derivative of $\bar{g}$ is given by

$$\dot{\bar{\boldsymbol{g}}} = \bar{\boldsymbol{R}}(\bar{\theta})\bar{\boldsymbol{u}} \tag{34.47}$$

with

$$\bar{\boldsymbol{u}} = \boldsymbol{A}(\alpha) \Big(\bar{\boldsymbol{R}}(f_\theta(\alpha)) \;\; -\partial f/\partial\alpha(\alpha) \Big) \begin{pmatrix} \boldsymbol{C}\boldsymbol{u} \\ \dot{\alpha} \end{pmatrix} \tag{34.48}$$

and

$$\boldsymbol{A}(\alpha) = \begin{pmatrix} I_2 & -S \begin{pmatrix} f_x(\alpha) \\ f_y(\alpha) \end{pmatrix} \\ 0 & 1 \end{pmatrix}. \tag{34.49}$$

From (34.47) and (34.48), one can view $\dot{\alpha}$ as a complementary control input that can be used to monitor the motion of the frame $\bar{\mathcal{F}}_{\mathrm{m}}(\alpha)$. More precisely, $\bar{\mathcal{F}}_{\mathrm{m}}(\alpha)$ can be viewed as an omnidirectional frame provided that $\bar{\boldsymbol{u}}$ can be rendered equal to any vector of $\mathbb{R}^3$, i. e., provided that the mapping $(\boldsymbol{u}, \dot{\alpha}) \longmapsto \bar{\boldsymbol{u}}$ is onto. Let us determine when this condition is satisfied. Equation (34.48) can also be written as

$$\bar{\boldsymbol{u}} = \boldsymbol{A}(\alpha)\boldsymbol{H}(\alpha)\begin{pmatrix}\boldsymbol{u}\\ \dot{\alpha}\end{pmatrix} \tag{34.50}$$

with

$$\boldsymbol{H}(\alpha) = \begin{pmatrix}\cos f_\theta(\alpha) & 0 & -\partial f_x/\partial\alpha(\alpha)\\ \sin f_\theta(\alpha) & 0 & -\partial f_y/\partial\alpha(\alpha)\\ 0 & 1 & -\partial f_\theta/\partial\alpha(\alpha)\end{pmatrix} . \tag{34.51}$$

Since $\boldsymbol{A}(\alpha)$ is invertible, $\bar{\mathcal{F}}_{\mathrm{m}}(\alpha)$ is omnidirectional if and only if the matrix $\boldsymbol{H}(\alpha)$ is also invertible. A function f which satisfies this property for *any* $\alpha \in S^1$ is called a *transverse function* [34.9]. The issue of the existence of such functions has been treated in the much more general context of the transverse function approach [34.8, 9]. In the present case, a family of transverse functions is given by:

$$f(\alpha) = \begin{pmatrix}\varepsilon\sin\alpha\\ \varepsilon^2\eta\frac{\sin 2\alpha}{4}\\ \arctan(\varepsilon\eta\cos\alpha)\end{pmatrix} \quad \text{with} \quad \varepsilon, \eta > 0 . \tag{34.52}$$

Indeed, with this function one can verify that, for any $\alpha \in S^1$, $\det\boldsymbol{H}(\alpha) = -\frac{\varepsilon^2\eta}{2}\cos(\arctan(\varepsilon\eta\cos\alpha)) < 0$. Note that the components of f uniformly tend to zero as ε tends to zero, so that the associated omnidirectional frame $\bar{\mathcal{F}}_{\mathrm{m}}(\alpha)$ can be made arbitrarily close to $\mathcal{F}_{\mathrm{m}}$ by choosing ε small (but different from zero).

Now, let $t \longmapsto \boldsymbol{g}_{\mathrm{r}}(t) = [\boldsymbol{x}_{\mathrm{r}}(t), \boldsymbol{y}_{\mathrm{r}}(t), \theta_{\mathrm{r}}(t)]^\top$ denote a smooth, but otherwise *arbitrary*, reference trajectory. It is not difficult to derive from (34.47) a feedback law $\bar{\boldsymbol{u}}$ which asymptotically stabilizes $\bar{\boldsymbol{g}}$ at $\boldsymbol{g}_{\mathrm{r}}$. A possible choice is given by

$$\bar{\boldsymbol{u}} = \bar{\boldsymbol{R}}(-\bar{\theta})[\dot{\boldsymbol{g}}_{\mathrm{r}} - k(\bar{\boldsymbol{g}} - \boldsymbol{g}_{\mathrm{r}})] , \tag{34.53}$$

which implies that $(\dot{\bar{\boldsymbol{g}}} - \dot{\boldsymbol{g}}_{\mathrm{r}}) = -k(\bar{\boldsymbol{g}} - \boldsymbol{g}_{\mathrm{r}})$ and therefore that $\bar{g} - g_{\mathrm{r}} = 0$ is an exponentially stable equilibrium of the above equation for any $k > 0$. Then, it follows from (34.46) that

$$\lim_{t\to+\infty}\left\{g(t) - g_{\mathrm{r}}(t) - \bar{\boldsymbol{R}}[\theta_{\mathrm{r}}(t)]f[\alpha(t)]\right\} = 0 . \tag{34.54}$$

The norm of the tracking error $\|\boldsymbol{g} - \boldsymbol{g}_{\mathrm{r}}\|$ is thus ultimately bounded by the norm of $f(\alpha)$ which, in view of (34.52), can be made arbitrarily small via the choice of ε. It is in this sense that practical stabilization is achieved. The control $\boldsymbol{u}$ for the unicycle-like robot is then calculated by inverting the relation (34.50) and using the expression (34.53) of $\bar{\boldsymbol{u}}$.

While it can be tempting to use very small values of ε for the transverse function f in order to obtain a good tracking precision, one must be aware of the limits of this strategy. Indeed, when ε tends to zero, the matrix $\boldsymbol{H}(\alpha)$ defined by (34.51) becomes ill-conditioned, and its determinant tends to zero. This implies, by (34.50), that the robot's velocities u_1 and u_2 may become very large. In particular, when the reference trajectory $\boldsymbol{g}_{\mathrm{r}}$ is not feasible, many manoeuvres are likely to occur. Note that this difficulty is intrinsic to the robot's nonholonomy and that it cannot be circumvented (think about the problem of parking a car in a very narrow parking place). For this reason, trying to impose very accurate tracking of nonfeasible trajectories is not necessarily a good option in practice. On the other hand, when the trajectory is feasible, manoeuvres are not needed to achieve accurate tracking, so that smaller values of ε can be used in this case. This clearly leads to a dilemma when the reference trajectory is not known in advance and its properties in term of feasibility can vary with time. A control strategy which addresses this issue, based on the use of transverse functions whose magnitude can be adapted online, is proposed in [34.10]. Experimental validations of the present approach on a unicycle-like robot can also be found in [34.11].

Car Case

The control approach presented above can be extended to car-like vehicles (and also to the trailer case). Again, the idea is to associate with the robot's frame $\mathcal{F}_{\mathrm{m}}$ an omnidirectional *companion* frame $\bar{\mathcal{F}}_{\mathrm{m}}(\alpha)$ which can be maintained arbitrarily close to $\mathcal{F}_{\mathrm{m}}$ via the choice of some design parameters. Let us show how this can be done for a car-like vehicle. To simplify the forthcoming equations, let us rewrite system (34.5) as

$$\begin{cases}\dot{x} = u_1\cos\theta ,\\ \dot{y} = u_1\sin\theta ,\\ \dot{\theta} = u_1\xi ,\\ \dot{\xi} = u_\xi ,\end{cases}$$

with $\xi = (\tan\phi)/L$ and $u_\xi = u_2(1+\tan^2\phi)/L$. This system can also be written as (compare with (34.45))

$$\begin{cases} \dot{\boldsymbol{g}} = \bar{\boldsymbol{R}}(\theta)\boldsymbol{C}(\xi)u_1\,, \\ \dot{\xi} = \boldsymbol{u}_\xi\,, \end{cases} \tag{34.55}$$

with $\boldsymbol{g} = (\boldsymbol{x}, \boldsymbol{y}, \theta)^\top$ and $\boldsymbol{C}(\xi) = (1, 0, \xi)^\top$. Let us now consider a smooth function

$$f : \alpha \longmapsto f(\alpha) = \begin{pmatrix} f_g(\alpha) \\ f_\xi(\alpha) \end{pmatrix} = \begin{pmatrix} f_x(\alpha) \\ f_y(\alpha) \\ f_\theta(\alpha) \\ f_\xi(\alpha) \end{pmatrix}$$

with $\alpha \in S^1 \times S^1$ (i. e. $\alpha = (\alpha_1, \alpha_2)$), and define (compare with (34.46))

$$\begin{aligned} \bar{\boldsymbol{g}} := \begin{pmatrix} \bar{x} \\ \bar{y} \\ \bar{\theta} \end{pmatrix} &:= \boldsymbol{g} - \bar{\boldsymbol{R}}(\theta - f_\theta(\alpha)) f_g(\alpha) \\ &= \begin{pmatrix} \begin{pmatrix} x \\ y \end{pmatrix} - \boldsymbol{R}(\theta - f_\theta(\alpha)) \begin{pmatrix} f_x(\alpha) \\ f_y(\alpha) \end{pmatrix} \\ \theta - f_\theta(\alpha) \end{pmatrix}\,, \end{aligned} \tag{34.56}$$

which, as in the unicycle case, can be viewed as the situation of some *companion* frame $\bar{\mathcal{F}}_\mathrm{m}(\alpha)$. By differentiating $\bar{\boldsymbol{g}}$ along any smooth time function $t \longmapsto \alpha(t)$ and any solution to system (34.55), one can verify that (34.47) is still satisfied, except that $\bar{\boldsymbol{u}}$ is now given by

$$\bar{\boldsymbol{u}} = \boldsymbol{A}(\alpha) \begin{pmatrix} \bar{\boldsymbol{R}}[f_\theta(\alpha)] & -\partial f_g/\partial\alpha_1(\alpha) & -\partial f_g/\partial\alpha_2(\alpha) \end{pmatrix} \times \begin{pmatrix} \boldsymbol{C}(\xi)u_1 \\ \dot{\alpha}_1 \\ \dot{\alpha}_2 \end{pmatrix} \tag{34.57}$$

rather than by (34.48) (with $\boldsymbol{A}(\alpha)$ still defined by (34.49)). Using the fact that

$$\begin{aligned} \boldsymbol{C}(\xi)u_1 &= \boldsymbol{C}(f_\xi(\alpha))u_1 + \{\boldsymbol{C}(\xi) - \boldsymbol{C}[f_\xi(\alpha)]\}u_1 \\ &= \begin{pmatrix} 1 \\ 0 \\ f_\xi(\alpha) \end{pmatrix} u_1 + \begin{pmatrix} 0 \\ 0 \\ \xi - f_\xi(\alpha) \end{pmatrix} u_1\,, \end{aligned}$$

(34.57) can also be written as

$$\bar{\boldsymbol{u}} = A(\alpha)\boldsymbol{H}(\alpha) \begin{pmatrix} u_1 \\ \dot{\alpha}_1 \\ \dot{\alpha}_2 \end{pmatrix} + A(\alpha) \begin{pmatrix} 0 \\ 0 \\ u_1[\xi - f_\xi(\alpha)] \end{pmatrix} \tag{34.58}$$

with

$$\boldsymbol{H}(\alpha) = \begin{pmatrix} \cos f_\theta(\alpha) & -\partial f_x/\partial\alpha_1(\alpha) & -\partial f_x/\partial\alpha_2(\alpha) \\ \sin f_\theta(\alpha) & -\partial f_y/\partial\alpha_1(\alpha) & -\partial f_y/\partial\alpha_2(\alpha) \\ f_\xi(\alpha) & -\partial f_\theta/\partial\alpha_1(\alpha) & -\partial f_\theta/\partial\alpha_2(\alpha) \end{pmatrix}\,. \tag{34.59}$$

By setting

$$\boldsymbol{u}_\xi = \dot{f}_\xi(\alpha) - k(\xi - f_\xi(\alpha)) \tag{34.60}$$

with $k > 0$, it follows from (34.55) that $\xi - f_\xi(\alpha)$ exponentially converges to zero. Hence, after some transient phase whose duration is commensurable with $1/k$, $\xi - f_\xi(\alpha) \approx 0$, and (34.58) reduces to

$$\bar{\boldsymbol{u}} = \boldsymbol{A}(\alpha)\boldsymbol{H}(\alpha) \begin{pmatrix} u_1 \\ \dot{\alpha}_1 \\ \dot{\alpha}_2 \end{pmatrix}\,. \tag{34.61}$$

Provided that the function f is such that $\boldsymbol{H}(\alpha)$ is always invertible, this latter relation means that the frame $\bar{\mathcal{F}}_\mathrm{m}(\alpha)$ associated with $\bar{\boldsymbol{g}}$ is omnidirectional. Any function f for which this property is satisfied is called a transverse function. Once it has been determined, one can proceed as in the unicycle case to asymptotically stabilize an arbitrary reference trajectory $\boldsymbol{g}_\mathrm{r}$ for $\bar{\boldsymbol{g}}$, for example, by defining $\bar{\boldsymbol{u}}$ as in (34.53). The control u_1 for the car is then obtained by inverting relation (34.61). The following lemma specifies a family of transverse functions for the car case.

Lemma 34.1

For any $\varepsilon > 0$ and any η_1, η_2, η_3 such that $\eta_1, \eta_2, \eta_3 > 0$ and $6\eta_2\eta_3 > 8\eta_3 + \eta_1\eta_2$, the function f defined by

$$f(\alpha) = \begin{pmatrix} \bar{f}_1(\alpha) \\ \bar{f}_4(\alpha) \\ \arctan(\bar{f}_3(\alpha)) \\ \bar{f}_2(\alpha)\cos^3 f_3(\alpha) \end{pmatrix}$$

with $\bar{f} : S^1 \times S^1 \longrightarrow \mathbb{R}^4$ given by

$$\bar{f}(\alpha) = \begin{pmatrix} \varepsilon(\sin\alpha_1 + \eta_2\sin\alpha_2) \\ \varepsilon\eta_1\cos\alpha_1 \\ \varepsilon^2\left(\frac{\eta_1\sin 2\alpha_1}{4} - \eta_3\cos\alpha_2\right) \\ \varepsilon^3\left(\eta_1\frac{\sin^2\alpha_1\cos\alpha_1}{6} - \frac{\eta_2\eta_3\sin 2\alpha_2}{4} - \eta_3\sin\alpha_1\cos\alpha_2\right) \end{pmatrix}$$

satisfies the transversality condition $\det\boldsymbol{H}(\alpha) \neq 0\,\forall\alpha$, with $\boldsymbol{H}(\alpha)$ defined by (34.59) [34.12].

The simulation results reported in Fig. 34.12 illustrate the application of this control approach for a car-like robot. The reference trajectory is defined by the initial condition $g_r(0) = 0$ and its time derivative

$$\dot{g}_r(t) = \begin{cases} (0,0,0)^\top & \text{if } t \in [0,30] \\ (1,0,0)^\top & \text{if } t \in [30,38] \\ (0,0.3,0)^\top & \text{if } t \in [38,53] \\ (-1,0,0)^\top & \text{if } t \in [53,61] \\ (0,0,0.2)^\top & \text{if } t \in [61,80] \end{cases}$$

This corresponds to a fixed situation when $t \in [0,30]$, three sequences of pure translational motion when $t \in [30,61]$, and a pure rotational motion when $t \in [61,80]$. Let us remark that this trajectory is not feasible for the car-like robot when $t \in [38,53]$, since it corresponds to a lateral translation in the direction of the unit vector $\boldsymbol{j}_r$ of the frame $\mathcal{F}_r$ associated with g_r, nor when $t \in [61,80]$, since a rear-drive car cannot perform pure rotational motion. The initial configuration of the car-like robot, at $t = 0$, is $\boldsymbol{g}(0) = (0, 1.5, 0)$, and the initial steering wheel angle is $\phi(0) = 0$.

In Fig. 34.12a, the robot is drawn with a solid line at several time instants, whereas the chassis of the reference vehicle is shown as a dashed line at the same time instants. The figure also shows the trajectory of the point located at the mid-distance of the robot's rear wheels. Figure 34.12b shows the time evolution of the tracking error expressed in the reference frame (i. e., (x_e, y_e) as defined by (34.20), and $\theta_e = \theta - \theta_r$). It follows from (34.54) that, after the transient phase associated with the exponential convergence of $\bar{g}$ to zero, the ultimate bound for $|x_e|$, $|y_e|$, and $|\theta_e|$ is upper-bounded by the maximum amplitude of the functions f_x, f_y, and f_θ, respectively. For this simulation, the control parameters of the transverse function f of Lemma 34.1 have been chosen as follows: $\varepsilon = 0.17$, $\eta_{1,2,3} = (12, 2, 20)$. With these values, one can verify that $|f_x|$, $|f_y|$, and $|f_\theta|$ are bounded by 0.51, 0.11, and 0.6, respectively. This is consistent with the time evolution of the tracking error in the figure. As pointed out for the unicycle case, a greater tracking precision could be obtained by decreasing the value of ε, but this would involve larger values of the control inputs and also more frequent manoeuvres, especially on the time intervals [38, 53] and [61, 80] when the reference trajectory is not feasible.

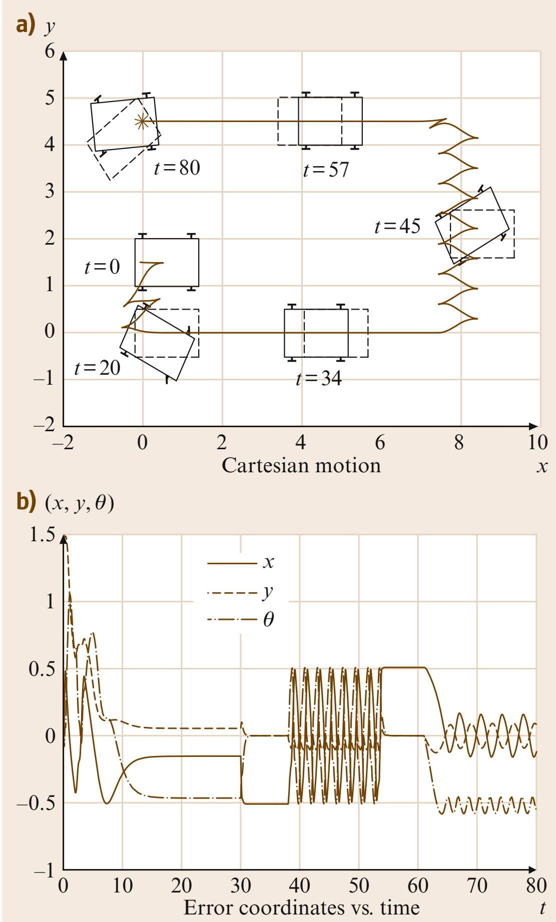

Fig. 34.12a,b Practical stabilization of an arbitrary trajectory by the transverse function approach

34.5 Complementary Issues and Bibliographical Guide

General Trailer Systems

Most of the control design approaches here presented and illustrated for unicycle-like and car-like vehicles can be extended to the case of trains of vehicles composed of trailers hitched to a leading vehicle. In particular, the methods of Sect. 34.4 which are specific to nonholonomic systems can be extended to this case, provided that the kinematic equations of motion of the system can be transformed (at least semiglobally) into a chained system [34.5]. This basically requires that the hitch point of each trailer is located on the rear-wheel axle of the preceding vehicle [34.13]. For instance, the transformation to the chained form is not possible when there are two (or more) successive trailers with off-axle hitch points [34.14]. So-called *general trailer systems* (with off-axle hitch points) raise difficult control design issues, and the literature devoted to them is sparse. For this reason, and also because these systems are not met in applications as frequently as simpler vehicles, control methods specifically developed for them are not reported here. Nonetheless, a few related references are given next. The path-following problem has been considered in, e.g., [34.15] for a system with two trailers and, more generally, in [34.16, Chap. 3] and [34.17] for an arbitrary number of trailers. To our knowledge, the problem of stabilizing non-stationary reference trajectories has not been addressed for these systems (except in the single trailer case for which the system can be transformed into the chained form [34.14, 18]). In fact, the explicit calculation of feasible trajectories joining a given configuration to another is already a very difficult problem, even in the absence of obstacles. As for the asymptotic stabilization of fixed configurations, the problem can (in theory) be solved by using existing general methods developed for the larger class of controllable driftless systems. However, the calculations associated with these methods quickly become intractable when the number of trailers increases. More specific and simpler ones have been proposed in [34.19], for an arbitrary number of trailers and the asymptotic stabilization of a reduced set of configurations, and in [34.20], in the case of two trailers and arbitrary fixed configurations.

Sensor-Based Motion Control

The control laws described in the present chapter, and their calculation, involve the online measurement, eventually complemented by the online estimation, of variables depending on the position of the vehicles in their environment. Measures can be acquired via the use of various sensors (odometry, GPS, proximetry, vision, ...). Usually, various treatments are applied to raw sensory data prior to computing the control variables themselves. For instance, noise filtering and state estimation are such basic operations, well documented in the automatic-control literature. Among all sensors, vision sensors play a particularly important role in robotic applications, due to the richness and versatility of the information which they provide. The combination of visual data with feedback control is often referred to as *visual servoing*. In Chap. 24, a certain number of visual servoing tasks are addressed, mostly in the context of manipulation and/or under the assumption that realizing the robot task is equivalent to controlling the pose of a camera mounted on an omnidirectional manipulator. In a certain number of cases, the concepts and methods described in this chapter can be adapted, without much effort, to the context of mobile robots. These cases basically correspond to the control methods adapted from robotic manipulation which are described in Sect. 34.3 of the present chapter. For instance, automatic driving via the control of the visually estimated lateral distance between a robotic vehicle and the side of a road, or car-platooning by controlling the frontal and lateral distances to a leading vehicle, can be addressed with the control techniques reported in Chap. 24. The reason is that it is possible to simply recast these techniques in the form of the control laws proposed in Sect. 34.3. However, there are also vision-based applications for nonholonomic mobile robots which cannot be solved by applying classical visual-servoing techniques. This is the case, for instance, of the task objectives addressed in Sect. 34.4, an example of which is the stabilization of the complete posture (i. e., position and orientation) of a nonholonomic vehicle at a desired one. Vision-based control problems of this type have been addressed in [34.10, 21].

A few former surveys on the control of WMRs have been published. Let us mention [34.22–24], which contain chapters on the modeling and control issues. A detailed classification of kinematic and dynamic models for the different types of WMR structures, on which Chap. 17 is based, is provided in [34.25]. The use of the chain form to represent WMR equations has been proposed in [34.26], then generalized in [34.13].

Path following may have been the first mobile robot control problem addressed by researchers in robotics. Among the pioneering works, let us cite [34.27, 28]. Several results presented in the present chapter are based on [34.5, 29].

The problem of tracking admissible trajectories for unicycle-type and car-like vehicles is treated in the books [34.22–24], and also in numerous conference and journal papers. Several authors have addressed this problem by applying dynamic feedback linearization techniques. In this respect, one can consult [34.30–32], and [34.22, Chap. 8], for instance.

Numerous papers on the asymptotic stabilization of fixed configurations have been published. Among them, [34.33] provides an early overview of feedback control techniques elaborated for this purpose, and also a list of references. The first result presenting a time-varying feedback solution to this problem, in the case of a unicycle-type vehicle, is in [34.3]. The conference paper [34.34] provides a survey on time-varying feedback stabilization, in the more general context of nonlinear control systems. More specific results, like Propositions 34.9 and 34.12, are given in [34.1, 5]. Other early results on the design of smooth time-varying feedbacks can be found in [34.35, 36], for example. Concerning continuous (but not Lipschitz-continuous) time-varying feedbacks yielding exponential convergence, one can consult [34.37]. Designs of hybrid discrete/continuous fixed-point stabilizers can be found in [34.38–40], for instance. The control law in Proposition 34.14 is taken from [34.6]. Discontinuous control design techniques are not addressed in the present chapter, but the interested reader will find examples of such feedbacks in [34.41, 42].

To our knowledge, the control approach presented in Sect. 34.4.6, which is based on the concept of transverse functions [34.8, 9], is the first attempt to address the problem of tracking *arbitrary* trajectories (i. e., not necessarily feasible for the controlled robot). Implementation issues and experimental results for this approach can be found in [34.10, 11]. An overview of trajectory tracking problems for wheeled mobile robots, with a detailed case study of car-like systems, is presented in [34.12].

References

34.1 P. Morin, C. Samson: Control of non-linear chained systems. From the Routh–Hurwitz stability criterion to time-varying exponential stabilizers, IEEE Trans. Autom. Control **45**, 141–146 (2000)

34.2 R.W. Brockett: Asymptotic stability and feedback stabilization. In: *Differential Geometric Control Theory*, ed. by R.W. Brockett, R.S. Millman, H.J. Sussmann (Birkauser, Boston 1983)

34.3 C. Samson: Velocity and torque feedback control of a nonholonomic cart, Proc. Int. Workshop Adapt. Nonlinear Control: Issues in Robotics (1990), also in LNCIS, Vol. 162, (Springer, Berlin, Heidelberg 1991)

34.4 J.-M. Coron: Global asymptotic stabilization for controllable systems without drift, Math. Control Signals Syst. **5**, 295–312 (1992)

34.5 C. Samson: Control of chained systems. Application to path following and time-varying point-stabilization, IEEE Trans. Autom. Control **40**, 64–77 (1995)

34.6 P. Morin, C. Samson: Exponential stabilization of nonlinear driftless systems with robustness to unmodeled dynamics, ESAIM: Control Optim. Calc. Var. **4**, 1–36 (1999)

34.7 D.A. Lizárraga: Obstructions to the existence of universal stabilizers for smooth control systems, Math. Control Signals Syst. **16**, 255–277 (2004)

34.8 P. Morin, C. Samson: Practical stabilization of driftless systems on Lie groups: the transverse function approach, IEEE Trans. Autom. Control **48**, 1496–1508 (2003)

34.9 P. Morin, C. Samson: A characterization of the Lie algebra rank condition by transverse periodic functions, SIAM J. Control Optim. **40**(4), 1227–1249 (2001)

34.10 G. Artus, P. Morin, C. Samson: Control of a maneuvering mobile robot by transverse functions, Proc. Symp. Adv. Robot Kinemat. (ARK) (2004) pp. 459–468

34.11 G. Artus, P. Morin, C. Samson: Tracking of an omnidirectional target with a nonholonomic mobile robot, Proc. IEEE Conf. Adv. Robotics (ICAR) (2003) pp. 1468–1473

34.12 P. Morin, C. Samson: Trajectory tracking for nonholonomic vehicles: overview and case study, Proc. 4th Int. Workshop Robot Motion Control (RoMoCo), ed. by K. Kozlowski (2004) pp. 139–153

34.13 O.J. Sørdalen: Conversion of the kinematics of a car with n trailers into a chained form, Proc. IEEE Int. Conf. Robot. Autom. (1993) pp. 382–387

34.14 P. Rouchon, M. Fliess, J. Lévine, P. Martin: Flatness, motion planning and trailer systems, Proc. IEEE Int. Conf. Decis. Control (1993) pp. 2700–2705

34.15 P. Bolzern, R.M. DeSantis, A. Locatelli, D. Masciocchi: Path-tracking for articulated vehicles with off-axle hitching, IEEE Trans. Control Syst. Technol. **6**, 515–523 (1998)

34.16 D.A. Lizárraga: Contributions à la stabilisation des systèmes non-linéaires et à la commande de véhicules sur roues. Ph.D. Thesis (INRIA-INPG, University of Grenoble, France 2000)

34.17 C. Altafini: Path following with reduced off-tracking for multibody wheeled vehicles, IEEE Trans. Control Syst. Technol. **11**, 598–605 (2003)

34.18 F. Lamiraux, J.-P. Laumond: A practical approach to feedback control for a mobile robot with trailer, Proc. IEEE Int. Conf. Robotics Autom. (1998) pp. 3291–3296

34.19 D.A. Lizárraga, P. Morin, C. Samson: Chained form approximation of a driftless system. Application to the exponential stabilization of the general N-trailer system, Int. J. Control **74**, 1612–1629 (2001)

34.20 M. Venditelli, G. Oriolo: Stabilization of the general two-trailer system, Proc. IEEE Int. Conf. Robot. Autom. (2000) pp. 1817–1823

34.21 M. Maya-Mendez, P. Morin, C. Samson: Control of a nonholonomic mobile robot via sensor-based target tracking and pose estimation, Proc. IEEE/RSJ Int. Conf. Intell. Robots Syst. (2006) pp. 5612–5618

34.22 C. Canudas de Wit, B. Siciliano, G. Bastin: *Theory of Robot Control* (Springer, Berlin, Heidelberg 1996)

34.23 J.-P. Laumond (Ed.): *Robot Motion Planning and Control*, Lect. Notes Control Inform. Sci., Vol. 229 (Springer, Berlin, Heidelberg 1998)

34.24 Y.F. Zheng (Ed.): *Recent Trends in Mobile Robots*, World Scientific Ser. Robotics Automat. Syst., Vol. 11 (World Scientific, Singapore 1993)

34.25 G. Campion, G. Bastin, B. d'Andréa-Novel: Structural properties and classification of kynematic and dynamic models of wheeled mobile robots, IEEE Trans. Robot. Autom. **12**, 47–62 (1996)

34.26 R.M. Murray, S.S. Sastry: Steering nonholonomic systems in chained form, Proc. IEEE Int. Conf. Decis. Control (1991) pp. 1121–1126

34.27 E.D. Dickmanns, A. Zapp: Autonomous high speed road vehicle guidance by computer vision, Proc. IFAC World Congr. (1987)

34.28 W.L. Nelson, I.J. Cox: Local path control for an autonomous vehicle, Proc. IEEE Int. Conf. Robot. Autom. (1988) pp. 1504–1510

34.29 C. Samson: Path following and time-varying feedback stabilization of a wheeled mobile robot, Proc. Int. Conf. Autom. Robot. Comput. Vis. (1992)

34.30 B. d'Andréa-Novel, G. Campion, G. Bastin: Control of nonholonomic wheeled mobile robots by state feedback linearization, Int. J. Robot. Res. **14**, 543–559 (1995)

34.31 A. De Luca, M.D. Di Benedetto: Control of nonholonomic systems via dynamic compensation, Kybernetica **29**, 593–608 (1993)

34.32 M. Fliess, J. Lévine, P. Martin, P. Rouchon: Flatness and defect of non-linear systems: introductory theory and examples, Int. J. Control **61**, 1327–1361 (1995)

34.33 I. Kolmanovsky, N.H. McClamroch: Developments in nonholonomic control problems, IEEE Control Syst. **15**, 20–36 (1995)

34.34 P. Morin, J.-B. Pomet, C. Samson: Developments in time-varying feedback stabilization of nonlinear systems, Proc. IFAC NOLCOS (1998) pp. 587–594

34.35 J.-B. Pomet: Explicit design of time-varying stabilizing control laws for a class of controllable systems without drift, Syst. Control Lett. **18**, 467–473 (1992)

34.36 A.R. Teel, R.M. Murray, G. Walsh: Nonholonomic control systems: from steering to stabilization with sinusoids, Int. J. Control **62**, 849–870 (1995), also in Proc. IEEE Int. Conf. Decis. Control (1992) pp. 1603–1609

34.37 R.T. M'Closkey, R.M. Murray: Exponential stabilization of driftless nonlinear control systems using homogeneous feedback, IEEE Trans. Autom. Control **42**, 614–6128 (1997)

34.38 M.K. Bennani, P. Rouchon: Robust stabilization of flat and chained systems, Proc. Eur. Control Conf. (1995) pp. 2642–2646

34.39 P. Lucibello, G. Oriolo: Stabilization via iterative state feedback with application to chained-form systems, Proc. IEEE Conf. Decis. Control (1996) pp. 2614–2619

34.40 O.J. Sørdalen, O. Egeland: Exponential stabilization of nonholonomic chained systems, IEEE Trans. Autom. Control **40**, 35–49 (1995)

34.41 A. Astolfi: Discontinuous control of nonholonomic systems, Syst. Control Lett. **27**, 37–45 (1996)

34.42 C. Canudas de Wit, O.J. Sørdalen: Exponential stabilization of mobile robots with nonholonomic constraints, IEEE Trans. Autom. Control **37**(11), 1791–1797 (1992)